OAK RIDGE NATIONAL LABORATORY LIBRARY
3 4456 0003930 3

ORNL/TM-9819

ornl

OAK RIDGE NATIONAL LABORATORY

MARTIN MARIETTA

Thermal Energy Storage Technical Progress Report April 1984–March 1985

J. F. Martin

OAK RIDGE NATIONAL LABORATORY
CENTRAL RESEARCH LIBRARY
CIRCULATION SECTION
4500N ROOM 175
LIBRARY LOAN COPY
DO NOT TRANSFER TO ANOTHER PERSON
If you wish someone else to see this report, send in name with report and the library will arrange a loan.

OPERATED BY
MARTIN MARIETTA ENERGY SYSTEMS, INC.
FOR THE UNITED STATES
DEPARTMENT OF ENERGY

Printed in the United States of America. Available from
National Technical Information Service
U.S. Department of Commerce
5285 Port Royal Road, Springfield, Virginia 22161
NTIS price codes—Printed Copy: A05; Microfiche A01

This report was prepared as an account of work sponsored by an agency of the United States Government. Neither the United States Government nor any agency thereof, nor any of their employees, makes any warranty, express or implied, or assumes any legal liability or responsibility for the accuracy, completeness, or usefulness of any information, apparatus, product, or process disclosed, or represents that its use would not infringe privately owned rights. Reference herein to any specific commercial product, process, or service by trade name, trademark, manufacturer, or otherwise, does not necessarily constitute or imply its endorsement, recommendation, or favoring by the United States Government or any agency thereof. The views and opinions of authors expressed herein do not necessarily state or reflect those of the United States Government or any agency thereof.

ORNL/TM-9819
Dist. Category UC-94a

Engineering Technology Division

THERMAL ENERGY STORAGE TECHNICAL PROGRESS REPORT
APRIL 1984—MARCH 1985

J. F. Martin

Date Published - January 1986

Prepared by the
OAK RIDGE NATIONAL LABORATORY
Oak Ridge, Tennessee 37831
operated by
MARTIN MARIETTA ENERGY SYSTEMS, INC.
for the
U.S. DEPARTMENT OF ENERGY
under Contract No. DE-AC05-84OR21400

OAK RIDGE NATIONAL LABORATORY LIBRARY
3 4456 0003930 3

CONTENTS

	Page
ABSTRACT	1
1. PROGRAM OVERVIEW	1
1.1 Industrial TES Systems	3
1.1.1 Composite high-temperature storage materials	3
1.1.2 Encapsulated metallic storage media	5
1.2 Building TES Applications	5
1.2.1 Dual-temperature clathrates	5
1.2.2 Dual-temperature ammoniates	6
1.2.3 Feasibility study of binary solutions	6
1.2.4 Ice/clathrate systems for seasonal applications	7
1.2.5 Gas clathrates for heat pump cool storage	7
1.2.6 Form-stable, high-density polyethylene	7
1.2.7 Mathematical modeling of a PCM packed bed system	8
1.2.8 Passive solar building modeling	8
1.2.9 Advanced passive solar building materials	9
1.2.10 Solid sensible heat storage	9
2. TECHNICAL PROGRESS — RESEARCH AND DEVELOPMENT PROJECTS	10
2.1 Generic Assessments	10
2.1.1 Dual-temperature clathrates	10
2.1.2 Dual-temperature ammoniates	11
2.1.3 Feasibility study of binary solutions	20
2.1.4 Liquid and solid solutions	33
2.2 TES Media Development	38
2.2.1 Gas clathrates for heat pump cool storage	38
2.2.2 Encapsulated metallic storage media	45
2.2.3 Composite high-temperature storage material	52
2.2.4 Form stabilization, high-density polyethylene	55
2.3 TES System Development	59
2.3.1 Ice/clathrate system for seasonal application	59
2.3.2 Advanced passive solar building materials	60
2.4 Technology Transfer of Solid Sensible Heat Storage Material	68
2.5 System Modeling	70
2.5.1 Passive solar building modeling	70
2.5.2 Mathematical modeling of a PCM system	73
3. SUMMARY AND CONCLUSIONS	78
REFERENCES	80

THERMAL ENERGY STORAGE TECHNICAL PROGRESS REPORT
APRIL 1984–March 1985

J. F. Martin

ABSTRACT

Progress in the development of Thermal Energy Storage (TES) technology under the Oak Ridge National Laboratory Thermal Energy Storage Program for the period April 1984–March 1985 is reported. The program goals and project structure are presented. Each of the areas of TES research active in the program is discussed, and a discussion of technology transfer efforts is included.

---

1. PROGRAM OVERVIEW

This report is on the progress made during the 1-year period April 1984–March 1985 by the Oak Ridge National Laboratory (ORNL) in the development of thermal energy storage (TES) technologies. Since 1976 ORNL has had responsibility for field management of various parts of the national program in TES. Presently, it has lead laboratory cognizance over building and industrial TES development. The ORNL program is conducted in consultation with, and with the concurrence of, the Department of Energy (DOE), Division of Energy Storage.

The overall program goal is to (1) develop the technology base required for efficient, cost-effective TES concepts in the areas of diurnal heating and cooling and industrial applications and (2) work with industry, universities, technical societies, and trade organizations to transfer the technologies to the private sector.

Specific objectives have been developed for selected critical, high-risk technology areas so that specific technical problems may be identified and program resources allocated in the most efficient manner. The objectives of the principal program elements and the associated benefits follow. Economic and technical targets that have been established in each program area are also shown.

1. Develop TES concepts for capture, storage, and reuse of high-temperature energy, which significantly increases the utilization of industrial reject heat.

   Benefit: Make economically feasible the conservation of the significant energy available from industrial waste heat.

   Targets: economic — $7500/10^6$ Btu installed cost (1982 dollars).

   technical — Storage temperatures of 177 to 1093°C (350 to 2000°F).

   Round-trip efficiency of 85%.

2. Develop TES concepts that allow heat pump thermal storage without degradation of overall heat pump performance.

   Benefit: Improved heat pump applicability to utility load control applications through performance that equals or exceeds nonstorage heat pump performance.

   Targets: economic — $6000/10^6$ Btu installed cost (1982 dollars).

   technical — Heat exchange effectiveness of >0.95 cool storage.

   Storage temperature of 4 to 10°C (40 to 50°F) cool storage, 32 to 35°C (90 to 95°F) hot storage.

3. Develop TES with ideal thermal response for passive solar building heating.

   Benefit: Improved existing passive solar storage systems that do not provide building temperatures in the ideal thermal comfort range.

   Targets: economic — $3300/10^6$ Btu installed cost (1982 dollars).

   technical — Raise level of stored energy utilized in the thermal comfort range by a factor of 10 over existing storage technology.

4. Research to advance the understanding of new TES materials and processes.

   Benefit: Maintain perspective on possibilities for advanced systems.

   Targets: economic — Assess projected system costs.

   technical — Determine physical and thermal properties and conceptual system descriptions.

5. Interact with private sector through technical societies, industry, and trade associations to evaluate research needs and effectively transfer the technologies developed.

   Benefit: The TES program justification is by transfer of developed technologies to industry for implementation.

   Targets: Wider recognition by the private sector of the value of thermal storage.

To meet these five objectives, a program that addresses the technical issues that impede the development of successful storage systems has been implemented by ORNL. The total program has been organized into work packages according to the work breakdown structure (WBS) shown in Fig. 1. As in previous years, not all of the categories of research were addressed in this year's project activity. Available resources were allocated to projects that, because of their promise of technical and economic viability, were deemed high priority. Summaries of the year's activities in those projects that were supported are provided in Sects. 1.1 and 1.2. These summaries are organized according to areas of application — industrial uses or building heating/cooling — and include all WBS categories in these two application areas.

1.1 Industrial TES Systems

1.1.1 Composite high-temperature storage materials (Project 2.6.1)

Under this project, techniques for fabricating heat storage pellets for direct-contact, heat-exchange charging/discharging in a packed bed have been developed. Research has centered on carbonate salts (Na_2CO_3 and Na_2CO_3-$BaCO_3$) supported and immobilized within the submicron-sized capillary structure of a sintered ceramic (MgO) matrix.

A low-cost, commercial-production-compatible pellet fabrication process has been developed and confirmed with production equipment. The components in fine powder form are mixed by dry vibratory milling. The addition of water to the mixed powder in a one part water to two parts powder by weight using a paddle mixer was found to improve pellet crack resistance upon sintering. The moist powder is dried at 150°C for 20 h,

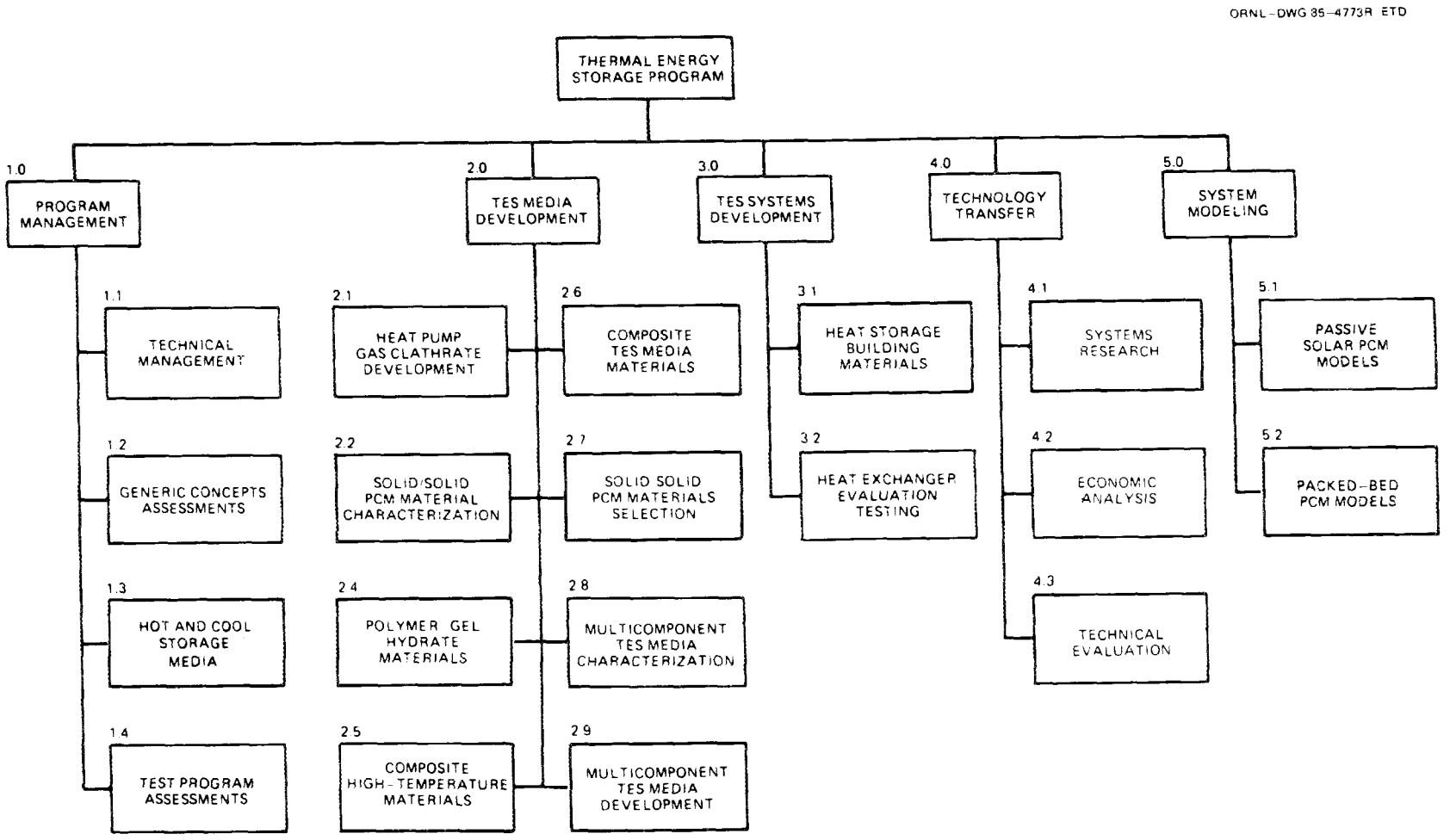

Fig. 1. TES Program work breakdown structure.

reducing water content to ~17%. Crack-free pellets pressed from this material and sintered at 1100°C for 1 h have been produced.

An applications/economic analysis of the use of this composite storage material in a periodic brick kiln operation is being conducted by an independent organization. Preliminary results show 300 × 10^6 Btu/cycle may be recovered for reuse in a one kiln—one dryer operation. This represents 30 × 10^9 Btu/year, and a simple payback period of 3 years has been calculated.

1.1.2 Encapsulated metallic storage media (Project 2.5.1)

Metallic eutectic alloys are potentially desirable TES media because their high thermal conductivity ensures rapid storage charge/discharge characteristics. However, successfully containing these systems has been a major obstacle to their use. To overcome this drawback, several methods of producing an integral shell of the high melting temperature component are under investigation. The material chosen for this initial study is a silicon-aluminum eutectic, the shell sought in this case being silicon that has both a high melt temperature and resistance to corrosion at high temperatures. The program has met with limited success in the initial scheme of producing a self-encapsulating shell by controlled cooling of a liquid hyper (rich in silicon) eutectic.

1.2 Building TES Applications

1.2.1 Dual-temperature clathrates (Project 1.3.1)

The possibility of utilizing materials that form clathrates at two temperatures was studied analytically and experimentally. The economic benefits of storage for heat pumps are significantly increased if both hot (winter) and cool (summer) storage can be obtained with a single storage system and a single storage medium. An existing crystallographic computer program was utilized to identify compounds that are stable in the correct temperature ranges for hot and cool storage. A bench-scale heat pump/storage loop was constructed to study the behavior of any promising systems under actual heat pump operating conditions. No viable

systems were found, and the projected effort in basic material behavior was judged to be beyond the resources of the TES program. Therefore, this project was concluded without follow-up research being defined.

1.2.2 Dual-temperature ammoniates (Project 1.3.2)

A number of inorganic salts undergo ammoniation reactions with gaseous or liquid ammonia (NH_3) that are analogous to hydration reactions. These ammoniation reactions may be suitable for latent heat storage at temperatures and pressures at which the ammoniate of the salt can be formed and decomposed. Two concepts were studied theoretically and experimentally. The first, found to be unfeasible, is a metallic salt (NaCl)-NH_3 system undergoing a pressure-sensitive liquid/solid transition. The second is similar to the clathrate system in that the refrigerant gas (ammonia) stores latent heat through singly or multiple complexing ammoniates in a crystallizer. The most promising metallic salt ammoniate, $NaCl \cdot n\ NH_3$, was examined, and its phase diagram at pressures above the NH_3 liquidus line was found to preclude obtaining satisfactory storage temperatures. A system based upon complexing of sodium bromide (NaBr) with ammonia was chosen as the most promising for further study in a prototype storage experiment.

1.2.3 Feasibility study of binary solutions (Project 1.3.3)

Conjugating binary (CB) solution is an attractive TES concept because only the liquid phase is involved. Several concepts are being studied: (1) a system with both an upper and lower critical solution temperature, (2) a system that forms a clathrate at a lower temperature and a solution at a higher temperature, and (3) a CB pair in which one of the fluids becomes supercritical when heated. Several promising systems have been identified. Experimental determination of the storage characteristics of such systems, however, remains to be implemented. One compound, propylene carbonate, was investigated analytically. Heat of mixing of propylene carbonate and water was estimated from existing mutual liquid-liquid solubility data and analytical representations of the composition and temperature variation of the activity coefficients of the

two components. Thus, an estimate of the storage capability of this system was determined and found to be promising.

1.2.4 Ice/clathrate systems for seasonal applications (Project 3.1.1)

A prototype seasonal ice storage system under investigation at Argonne National Laboratory (ANL) is based upon a heat pipe using refrigerant R-12 to make ice throughout the winter season for summer air conditioning. The feasibility of an ice/clathrate hybrid system was investigated. The economics of such a system, however, were found to be less favorable than that of a pure ice storage system.

1.2.5 Gas clathrates for heat pump cool storage (Project 2.1.1)

Ice-like gas clathrates have been shown to have potentially superior performance over ice as a cool storage medium. The higher freezing temperatures available with clathrates of the common fluorocarbon refrigerants are favorable to heat pump capacity, as well as to the coefficient of performance (COP). These materials have latent heats of fusion that are comparable to that of ice, thus maintaining the low storage volume advantage of latent heat storage. Use of the heat pump refrigerant as a component of the storage medium allows the possibility of direct-contact heat transfer into storage, which results in the increased efficiency of the heat pump cycle. The continuing investigation of these materials focused on clathrates of mixed refrigerants. By proper combination of refrigerant R-11 and R-12, both the pressure and temperature at which the clathrate forms have been optimized for the most efficient and economical storage systems.

1.2.6 Form-stable, high-density polyethylene (Project 2.7.1)

Field studies of solar heat storage in cross-linked polyethylene, a material previously developed under the TES program, showed deficiencies in material characteristics. The radiation cross-linking of polyethylene pellets results in a semisolid state of the "melted" pellet, thus rendering the material suitable for use in a packed bed heat storage vessel

that allows direct-contact heat exchange into and out of storage. The degree of cross-linking that is related to the starting material and radiation dose can be adjusted to increase the form stability of the melted phase of the material. Studies were conducted to optimize the radiation condition variables, as well as to compare electron beam with gamma ray radiation on the processed pellets' thermal performance.

1.2.7 Mathematical modeling of a PCM packed bed system (Project 5.2.1)

An analytical description of two-phase flow in a packed bed heat exchanger was developed in a previous program year. The system consists of direct-contact heat exchange between an evaporating/condensing heat-exchange fluid (refrigerant) and latent heat storage material that is pelletized and encapsulated to accommodate the packed bed environment. An experimental program, which utilizes the phase change material (PCM) pellets developed under a previous ORNL TES program subcontract (in conjunction with the analytical effort), was completed. Data obtained were used to validate the accuracy of the model.

1.2.8 Passive solar building modeling (Project 5.1.1)

A computer simulation code, PCMSOL-1, for a direct-gain, passive solar structure incorporating latent heat storage components has been developed by ORNL. It simulates in small time steps the temperature and phase state of each storage component of a building. It substantially extends the simulation capabilities of previous codes and incorporates PCM storage and heat exchange with the sun (via direct and diffuse gain), the sky (via sky radiation), and the surrounding ambient air (via convection) and among its own elements (via radiation between walls, conduction heat transfer within the structure, and heat exchange between interior air and surfaces). Experiments in a passive solar test chamber are being conducted to provide validating data for this code. In addition, the data are being used as indicators of improvements that can be incorporated into PCMSOL-1 to provide a more realistic simulation of passive heating from storage.

1.2.9 Advanced passive solar building materials (Project 3.1.2)

The concept of incorporation of PCM into building materials has received increasing attention because it provides an attractive alternative to the use of aggregate construction for the addition of thermal mass. The PCM concept lends itself to lightweight, low-volume construction techniques that are more closely related to standard building practices. Past research has revealed, however, several problems that must be addressed before incorporation of PCM into building materials is successful: (1) incongruent melting of PCM, (2) nucleation requirements, (3) vapor transmission through container, and (4) corrosiveness of PCM. These problems were addressed in the experimental program completed this year. A feasible system of passive storage based upon the concept of replacing the interior surface material (i.e., wallboard) of a passive solar room with panels filled with a latent heat storage medium has been demonstrated. Additional improvements in the latent heat material are required before the concept can be considered for commercialization, however.

1.2.10 Solid sensible heat storage (Project 4.3.1)

A project of development of castable olivine TES bricks for residential storage furnaces was completed. Reductions in media costs because of the use of domestically available raw materials, a less energy-intensive manufacturing process, and the production of a media with increased thermal capacity and increased lifetime were sought.

Olivine castables were developed with calcium aluminate cement and with sodium polyphosphate binders. Tests were conducted on storage bricks containing millscale (magnetite) as a density- and heat-capacity-increasing material. A monolithic cement-bonded section containing a cast-in-place heating element was tested.

It was shown that inexpensive, relatively simple technology involving olivine concretes is feasible and provides opportunity for small business to participate in the TES industry through utilization of this technology.

2. TECHNICAL PROGRESS — RESEARCH AND DEVELOPMENT PROJECTS

The major emphasis during this reporting year was on the development of TES materials that could be adapted to systems that will provide superior heat transfer performance and also materials that exploit previously undeveloped phase transitions to achieve greater storage efficiency and dual-temperature storage capability.

2.1 Generic Assessments

A thorough search of phase change systems that might find use as storage media was conducted. Two areas were covered: heats of hydration and heats of mixing. The approach was to examine a large range of possible systems, using an understanding of the fundamental phase change properties of the materials. As a result, the systems found promising probably represent those available for serious consideration as storage media.

2.1.1 Dual-temperature clathrates (Project 1.3.1)

Preliminary experiments[1] were conducted to determine the effects of additives to water/refrigerant R-12 systems on the upper invariant quadruple point Q_2 of clathrate formation. There are hydrate systems, similar to the freon/water systems, known for various alkyl ammonium salts in which the anion is bound into the water cage and the alkyl ammonium cation is encapsulated.

It was projected that combining alkyl ammonium salts with R-12 would provide additional stabilization of the hydrate clathrate because of both the salt binding into the framework of the clathrate and the effect of alkyl chains holding it together by intertwining the cavities of the hydrate framework.

Studies of the effect of chain length of the salt with the anion kept constant were carried out. Varying the length of the chain was accomplished by additions in turn of tetramethyl ammonium, tetraethyl ammonium, and tetra-η-butyl ammonium while keeping the anion constant as

iodine. The progressively higher chain lengths showed the desired effect on both Q_1 and Q_2, the tetra-η-butyl ammonium giving Q_1 of 8.5°C and Q_2 of 16.5°C.

Substitution of F^- for I^- as the anion accomplished the expected increase in Q_2. This is due to the increase in H-bonding strength of F^- over I^-. The results using tetramethyl ammoniate were not consistent; however, tetra-η-butyl ammoniate gave an increase of Q_2 from 16.5 to 22°C. Fluoride is not a practical material for commercial heat pump systems, however.

Additional experiments with sulphonates as the anion were conducted. There was no change in the temperature of the Q_2 point when p-toluenesulphonate was substituted for I in tetraethyl ammoniate, although the sulphonate might be expected to deform and, thus, weaken the hydrate lattice. The use of sulphonates would be desirable because of their low toxicity and availability as surfactants.

A final study compared trimethylphenol ammoniate bromide with the previous tetramethyl ammoniate iodide system. The result was a significant increase in Q_2 from 13 to 17°C.

None of the results with R-12 gave a Q_2 temperature high enough for heat storage. Much additional work remains before the success of the useful modification of the clathrate characteristic with additives can be judged.

2.1.2 Dual-temperature ammoniates (Project 1.3.2)

Complex compounds under investigation for dual-temperature energy storage consist of a metal-inorganic salt as the central atom and a ligand — such as NH_3, H_2O, or methanol — that is coordinated around the salt atom. The most common complexes are hydrates and ammoniates with water and ammonia as the ligand(s). The thermochemical reaction between the solid salt and the gaseous ligand cycles from an endothermic phase to an exothermic phase. Exothermically, the heat evolution during the adsorption of the ligand gas is used for heating purposes. The endothermic desorption reaction yields the refrigeration cycle.

Because of different vapor pressures for different complexes and ligands, the reaction between two paired complexes or one complex and the

plain ligand proceeds without an external driving force. The reverse reaction, the charging process, is performed with a gas compressor during off-peak power periods. Since both processes, charging and discharging, are exploited for cooling or heating, the system can be operated as a monovalent heat pump.

The main advantage of complex compounds over conventional working fluids such as freons or alcohols is the superior reaction energy generated compared with that produced by the mere condensation or evaporation process. The heat evolution and dissociation energies in the air-conditioning temperature range are 70 to 90% higher than the respective phase change of the pure ligand.

Two concepts have been evaluated. Concept A, utilizing a singly complexing ammoniate, is illustrated in Fig. 2. Storage temperature levels are determined by the operating pressure in the cylinder, and phase behavior is that occurring across the complexing line above the NH_3 liquidus line so that a solid-liquid reaction is obtained. Data in the

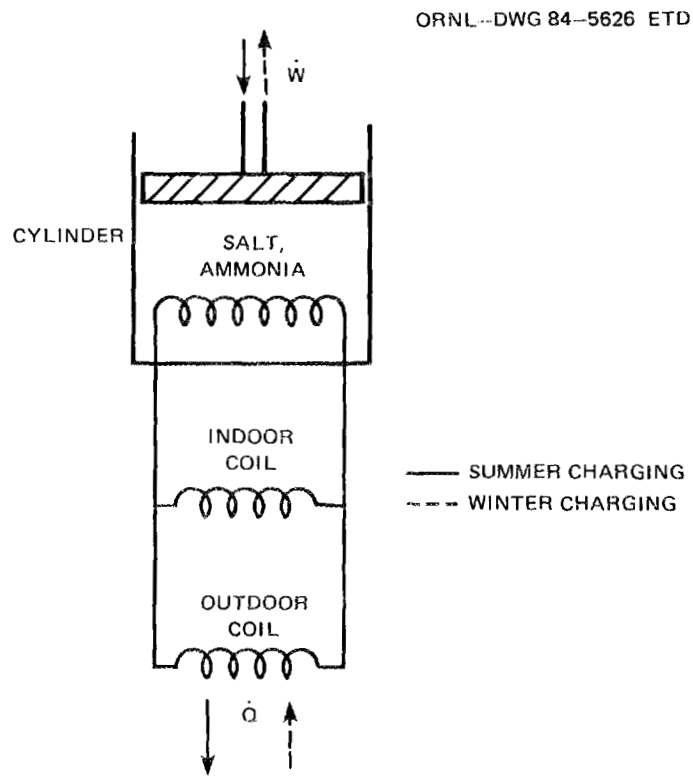

Fig. 2. Concept A — dual-temperature storage system.

desired region were obtained for $NaCl \cdot n\ NH_3$, the only compound that has a coordination step in the liquid phase at a temperature of interest for heat pump storage. The equilibrium line, determined as shown in Fig. 3, has the wrong slope, and complexing above a temperature of −9.6°C cannot be achieved.

Concept B, illustrated in Fig. 4, requires multiple complexing ammoniates with suitable transition temperatures obtainable by variation of storage pressure. One hundred seventy-nine ammine complexes were evaluated for their applicability to a storage system based upon this concept. Five were selected for experimental study:

$LiCl \cdot 3\text{–}4\ NH_3$

$NaBr \cdot 0\text{–}5\ NH_3$

$CaCl_2 \cdot 4\text{–}8\ NH_3$

$BaCl_2 \cdot 0\text{–}8\ NH_3$

$CaF_2 \cdot H_2O \cdot 1\text{–}5\ NH_3$

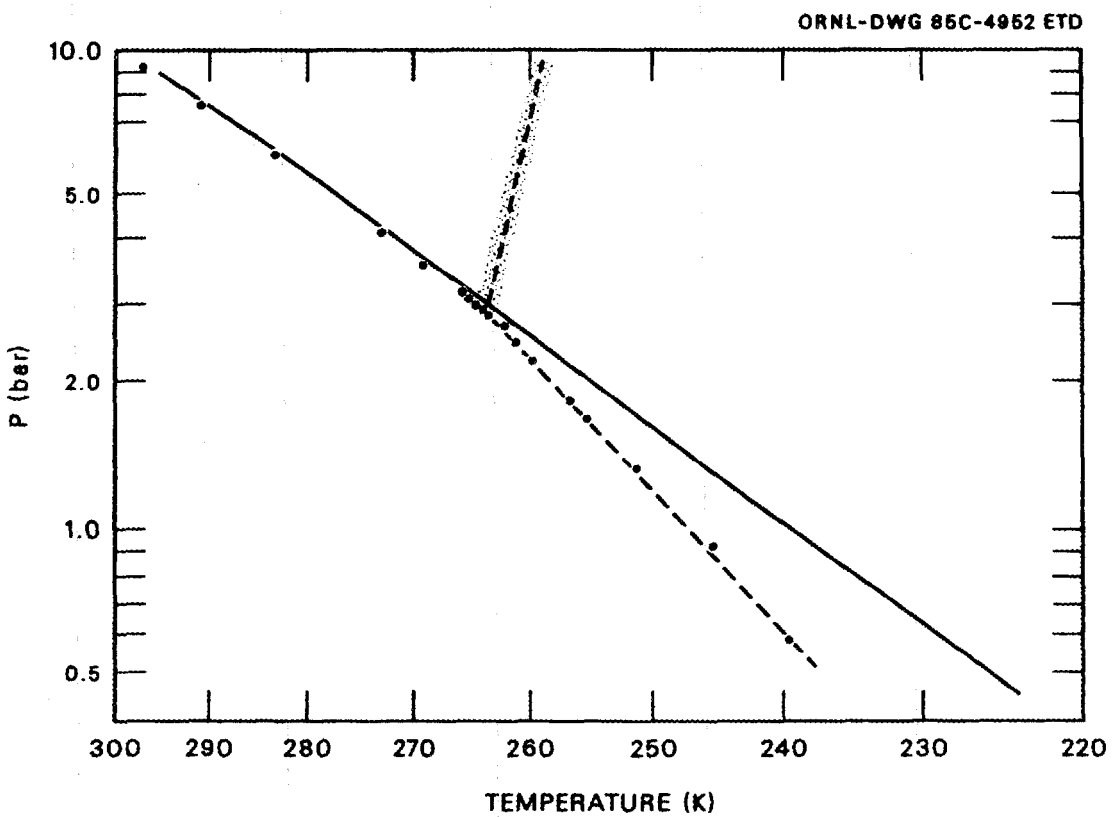

Fig. 3. Vapor pressure of $NaCl \cdot n\ NH_3$.

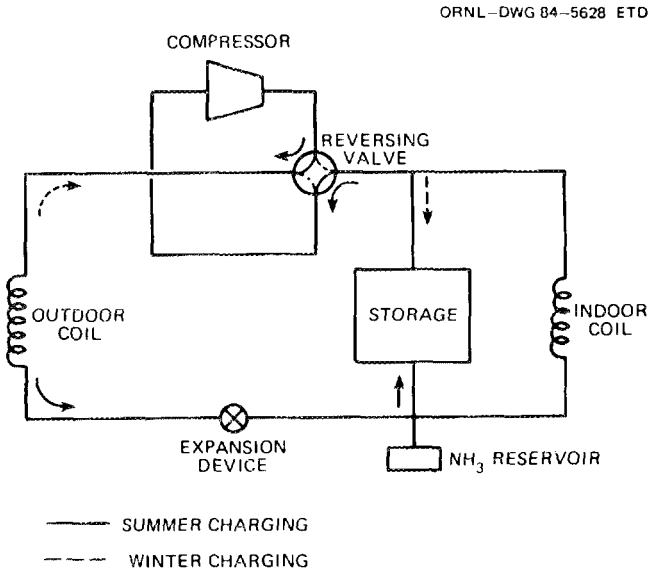

Fig. 4. Concept B — dual-temperature storage system.

These materials were studied to determine, as required, energy density, chemical stability, and appropriate ammoniation steps. In addition, toxicity was a consideration for further selection.

Figure 5 depicts a system with options for heating or cooling during both charging and discharging of storage. During the heating season, off-peak charging of storage is by desorption of NH_3 through operation of the compressor. The building is heated by the condenser coil as in a conventional heat pump system. On-peak heating is through the heat evolved by complex formation. NH_3 flows from the storage vessel through the evaporator coil to the salt storage vessel.

Summer off-peak charging is similar to building cooling by the desorption process and heat rejection by the condenser coil. On-peak cooling is by the discharge of storage through the evaporator coil.

The addition of a ground heat exchanger will improve the overall efficiency of the system. Figure 6 shows the use of the relatively constant temperature present in the ground on the several operating modes of the system. Availability of a suitable area for a ground heat exchanger, as well as the economic trade-off between increased performance and increased cost, must be considered.

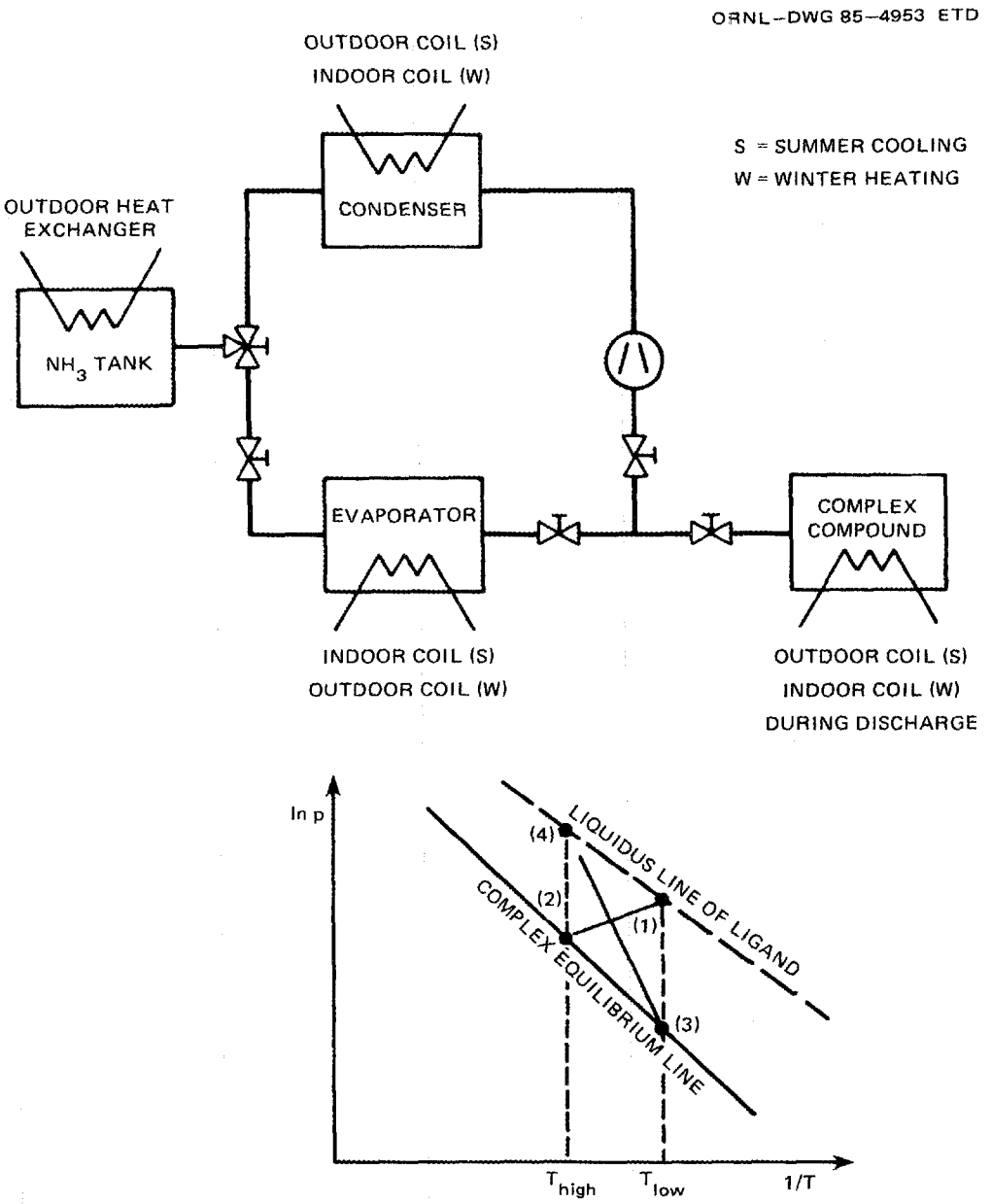

(1) → (2) DISCHARGING = HEATING WITH COMPLEX COMPOUND AND COOLING WITH LIGAND
(3) → (4) OFF-PEAK CHARGING

Fig. 5. Monovalent storage system.

Several conceptual designs are possible for the application of the substances investigated under concept B. The valence of the system is one of the major criteria for the selection of the concept. A monovalent heat pump is a stand-alone system; a bivalent heat pump, however, requires a supplemental heat source under certain ambient conditions.

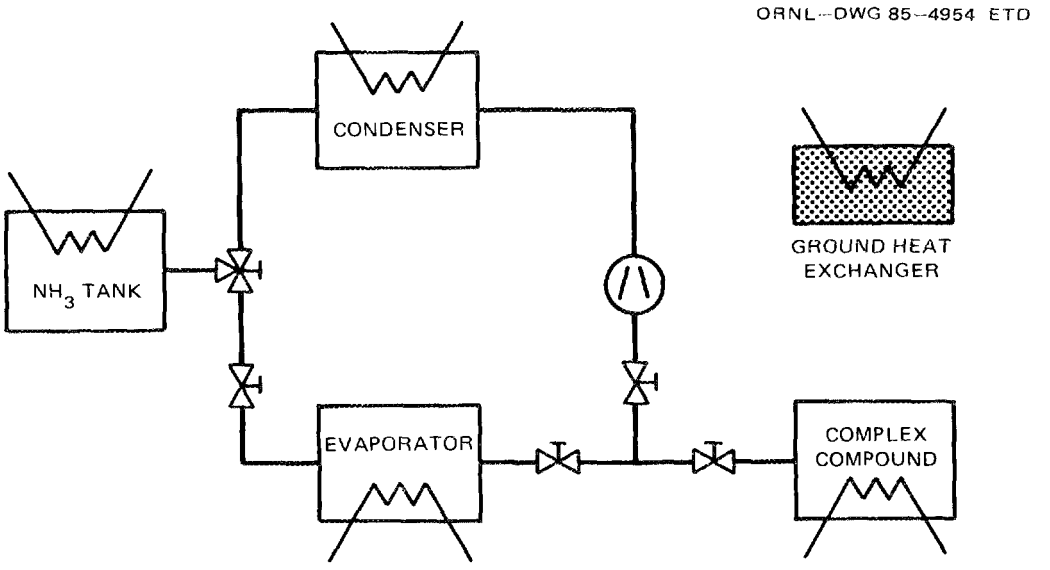

	SUMMER COOLING		WINTER HEATING	
	DISCHARGE	CHARGE	DISCHARGE	CHARGE
NH_3 TANK	–	GROUND HEAT EXCHANGER	GROUND HEAT EXCHANGER	–
CONDENSER	–	GROUND HEAT EXCHANGER	–	INDOOR COIL
EVAPORATOR	INDOOR COIL	–	GROUND HEAT EXCHANGER	–
COMPLEX CONTAINER	GROUND HEAT EXCHANGER	INDOOR COIL	INDOOR COIL	GROUND HEAT EXCHANGER

Fig. 6. Monovalent storage system with ground heat exchanger.

If the heat pump/storage system is to be operated as a bivalent system together with a conventional heater or air conditioner, the technical requirements are low compared with those of monovalent operation. On the other hand, since the heat pump elements such as the compressor, evaporator, condenser, expansion valve, reaction container, and ligand container are necessary for both operational modes, the capital investment for a monovalent heat pump/storage system will be considerably lower than for a bivalent system.

The thermodynamic requirements of the working fluid are easier to fulfill with the bivalent system. The efficiency of the heat pump is approximately the same for monovalent and bivalent operation at moderate temperature conditions. In extreme weather conditions, when the bivalent system switches to the conventional heater or cooler, the COP of the

monovalent system decreases, but it still remains in the heat pump mode with a COP >1.

Although the requirements for the working fluid are more difficult to fulfill, the program first concentrated on a monovalent design since in the research and development of the last 5 to 10 years, numerous bivalent systems that never entered the market because of the required high capital investment have been developed.

The following requirements were assumed:

1. operation of the machine in heating and cooling mode,
2. operation from −25 to +45°C ambient temperature,
3. off-peak storage capability from 7 to 37°C or better ambient temperature, and
4. off-peak cooling *and* heating capability in the temperature range of No. 3.

In some applications, however, the capability of off-peak heating and cooling is not necessary. Design changes for such applications should not cause major hardware reconstruction. The system must be easy to adapt, and the COP should increase with decreasing heating or cooling loads.

If groundwater, a lake, or a river is available, the outdoor heat exchanger should be connected to these sources. Ground heat exchangers are also possible if there is no water available. The capital investment for this type of heat exchanger, however, is very high. Figure 6 depicts a concept of a monovalent system with a ground heat exchanger. The ground temperature is assumed to be 15°C ± 2°C. The disadvantage of a costly ground heat exchanger is offset by the advantage of a moderate temperature lift. The design allows for off-peak heating and cooling. The regular heat pump cycle guarantees conventional operation and avoids shutdown periods necessary to reach the new operation temperatures in the reaction and ligand container after the completion of the adsorption or desorption. Space heating systems, however, are usually sluggish, and their heat capacity can allow a moderate shutdown period. A promising working fluid for this concept based on a ground heat exchanger is $NaBr \cdot n NH_3$.

A concept that can operate without a ground heat exchanger is depicted in Fig. 5. The thermodynamic requirements are much higher than for the previous designs because an intermediate temperature of 15°C is not available. Thus, the heat pump must provide the full temperature lift between the evaporator and the condenser. Possible working fluids for the design as depicted in Fig. 5 are $CaCl_2 \cdot n\ NH_3$, $NaI \cdot n\ NH_3$, and $BaCl_2 \cdot n\ NH_3$. Calcium chloride (CaCl) and sodium iodide (NaI) have very good off-peak heating and cooling characteristics. The charging process — desorption of the complex — however, requires a high-pressure lift if the complex is to be exploited for cooling and heating purposes during this phase.

Figure 7 depicts the dichotomy of the pressure levels in a heat pump. For an off-peak operation a pressure difference of ~0.7 to 1 bar is needed between $P_{low\ 2}$ and $P_{high\ 1}$. The further the vapor pressures of the respective substances (substance 1 and substance 2) are apart, the better the off-peak operation but the less efficient the charging. There are two possible solutions to this problem:

1. optimize the pressure relation by finding the ideal substance or
2. use the conventional cycle during the charging and maintain a certain temperature in the reaction vessel by utilizing the compressor heat.

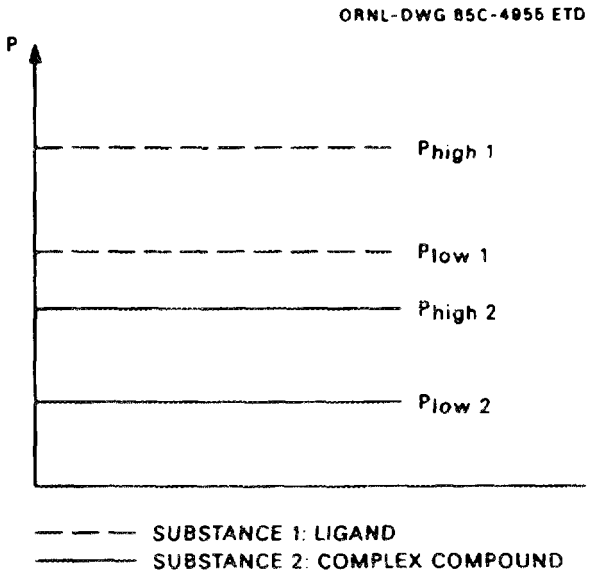

Fig. 7. Pressure levels of complex-compound heat pump.

For the optimization of the pressure relation, substances with a higher vapor pressure than $CaCl_2 \cdot n\ NH_3$ and a lower vapor pressure than $NaBr \cdot n\ NH_3$ have to be found. Therefore, NaI was investigated. Its vapor pressure is slightly higher than $CaCl_2$, but, unfortunately, the increase over $CaCl_2$ is not as high as predicted by Nernst.[2] A search for a more suitable substance is continuing.

The concept chosen, however, does not require any intermediate temperature and, therefore, no ground heat exchanger. A modification of this concept, depicted in Fig. 8, allows the compressor to be used for adsorption and desorption processes. This further allows for an adsorption reaction with $NaBr \cdot n\ NH_3$ even at extreme temperatures. The power requirements of the discharge process, however, will not be equal to zero but will use some input.

Figure 9 depicts the power requirements for this concept and the resulting modification. The higher versatility of the modified concept, which guarantees an operation even at extreme temperatures, will serve the load leveling at all weather conditions. Therefore, the decision of when to switch to the conventional NH_3 cycle without storage capability can be based on the process efficiency rather than the thermodynamic limits of the chemical reaction.

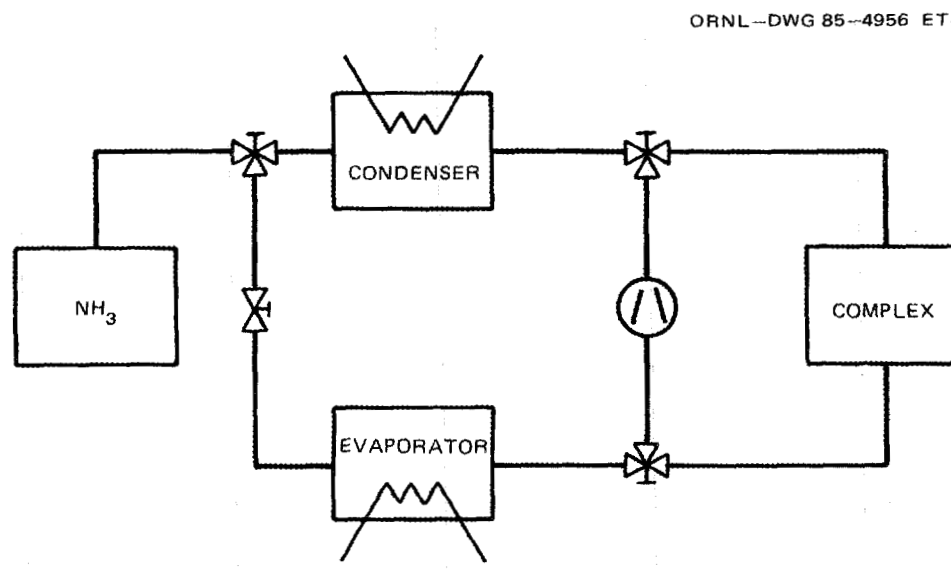

Fig. 8. Modified heat pump storage concept.

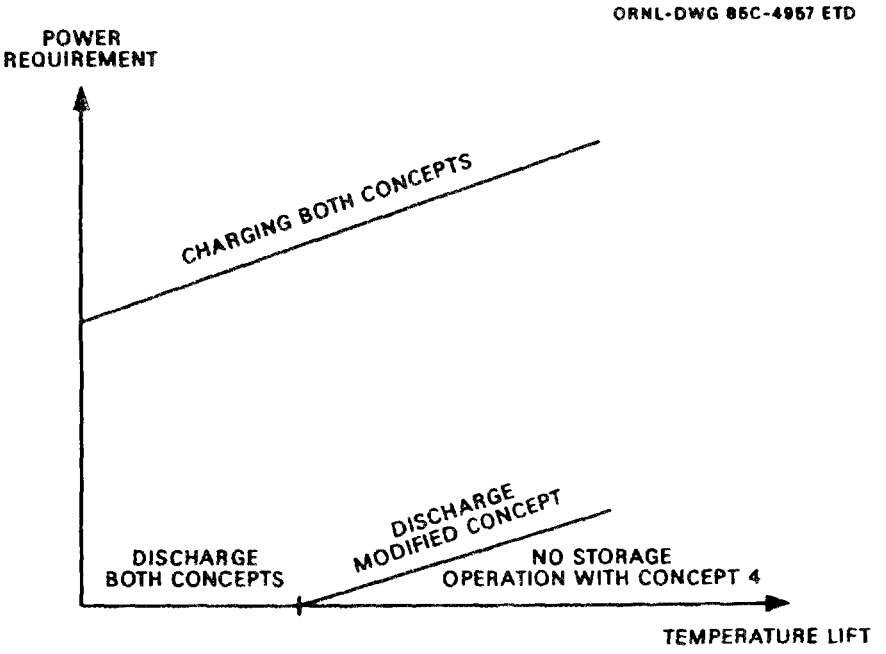

Fig. 9. Power requirements.

In addition to the concepts using one complex and the plain ligand, two paired complexes also can be exploited in a heat pump storage concept (see Fig. 10). The disadvantage of shutdown times of ~10 min between each adsorption and desorption can be overcome by two alternately operating container systems.

Possible working media pairs can be composed with $NaBr \cdot n\ NH_3$ as the high-pressure substance and $CaCl_2 \cdot n\ NH_3$ or $NaI \cdot n\ NH_3$ as the low-pressure substance.

This system can also be operated with plain NH_3 as the high-pressure substance. An additional condenser/evaporator heat exchanger increases the efficiency because heat capacity losses in the ammonia tank can be avoided.

The efficiency improvement of a ground heat exchanger, optional for all systems, is being examined with a computer simulation.

2.1.3 Feasibility study of binary solutions (Project 1.3.3)

Four categories of CB solutions were investigated and assessed for practical dual-temperature heat storage systems.[3] The categories were

ORNL–DWG 85–4958 ETD

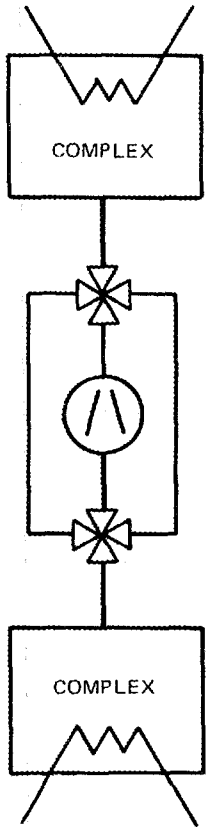

Fig. 10. Concept using two paired ammoniated salts.

CBs capable of clathration and/or monotectic reaction, closed-loop CBs, liquid or supercritical gas CBs, and high-temperature CBs.

CBs that undergo endothermic solution (hill-type CB behavior) at the higher temperature clathrate and/or monotectic reaction at the lower temperature appear most likely to be adaptable to practical dual-temperature TES for applications such as building heating and cooling. An economic analysis of a representative CB in this category for load-leveling applications indicates promise. In the high-temperature range, the CB-monotectic system Na-NaCl compares favorably economically with systems based on sensible and latent heat of fusion systems. Enhanced heat transfer rates because of avoidance of crystal growth on heat transfer surfaces during clathrate/monotectic or CB phase change should considerably improve these preliminary economic projections for CB systems.

The study also identified the CB-clathrate/monotectic systems of propylene carbonate plus water and sulfur dioxide plus water that may be of eventual practical interest.

Prior work on CBs has indicated that CBs are potentially very promising for TES applications.[4,5] The present study concerned itself in four categories with searches for practical CB systems and economic assessments of promising candidates:

1. CBs capable of clathration or monotectic reaction. Systems in this category would undergo clathration or monotectic reactions in the 5 to 10°C range and exhibit conjugation in the 30 to 50°C range.
2. Closed-loop CBs with lower and upper critical solution temperatures (CSTs) in the 5 to 10°C and 30 to 50°C ranges, respectively.
3. CB systems utilizing either liquid or supercritical gases. Such systems may possess exceptionally high heats of mixing because of low molecular weights and unusual physical states.
4. CBs for high-temperature applications.

In a prior initial study of CB feasibility for heat storage,[4] the steps needed to calculate the amount of heat stored over a temperature interval were indicated. The total heat absorbed or liberated over a temperature interval from some temperature T_1 below the CST to some temperature T_2 above the CST (Fig. 11) consists of the following terms:

$$\Delta H_{T_1 \to T_2} = (n_a + n_b)\, \Delta H_{M,T_c} - (n_a' + n_b')\, \Delta H'_{M,T_1} - (n_a'' + n_b'')\, \Delta H''_{M,T_1} + (n_a C_{P_a} + n_b C_{P_B})\, (T_c - T_1) + (n_a + n_b)\, C_{P_{soln}}\, (T_2 - T_c)\ , \quad (1)$$

where

ΔH_M = heat of mixing,

C_p = heat capacity,

n_a, n_b = number of moles of components A and B,

primes = values of the above as mole fractions X, X′, and X″ (as shown in Fig. 11).

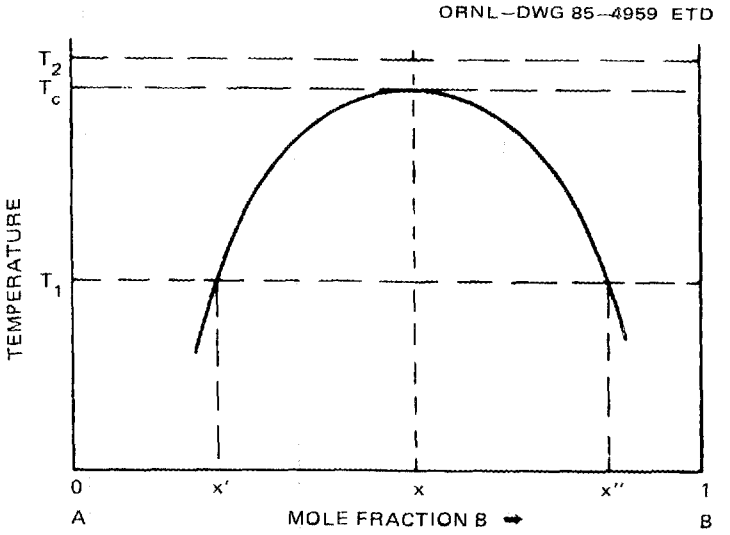

Fig. 11. Phase diagram for hill-type CB.

Equation 1 indicates that the total heat of mixing over a temperature interval $T_1 \rightarrow T_2$ may be more or less than the heat of mixing at T_c, depending on the signs and magnitudes of the heats of mixing and the degree of separation at T_1. The contributions of the heat capacity terms are expected to be of minor significance over small temperature intervals.

Heats of mixing at compositions greatly removed from the composition at the CST are generally very small. Thus, the necessity of having a CB phase diagram (Fig. 12) of Type 1, as opposed to Type 2, is reemphasized (Ref. 4).

Heat of mixing values as a function of temperature can vary in several ways, depending on the particular pair and concentration of components involved. Alcohols with water, for example, show heats of mixing that actually change sign depending on concentration (Fig. 13). Unfortunately, data on heats of mixing as a function of temperature and concentration are very scarce.

An overall idea of the storage behavior of a CB system can be gained from consideration of the C_p vs temperature curve. A few C_p vs temperature curves for some CBs have appeared in the literature (e.g., Refs. 6 and 7). The form of the curves is generally shown in Fig. 14. From a

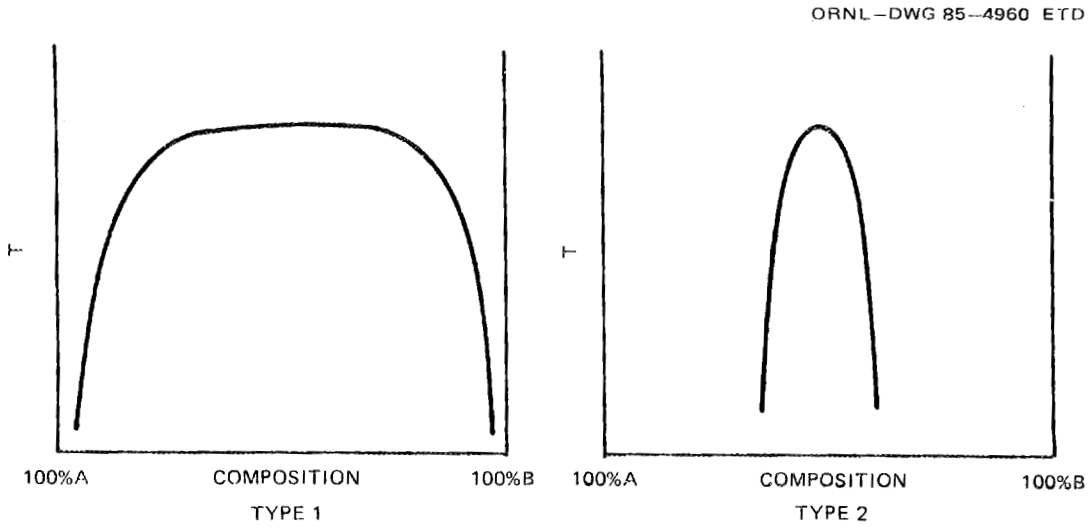

Fig. 12. Types of CB phase diagrams.

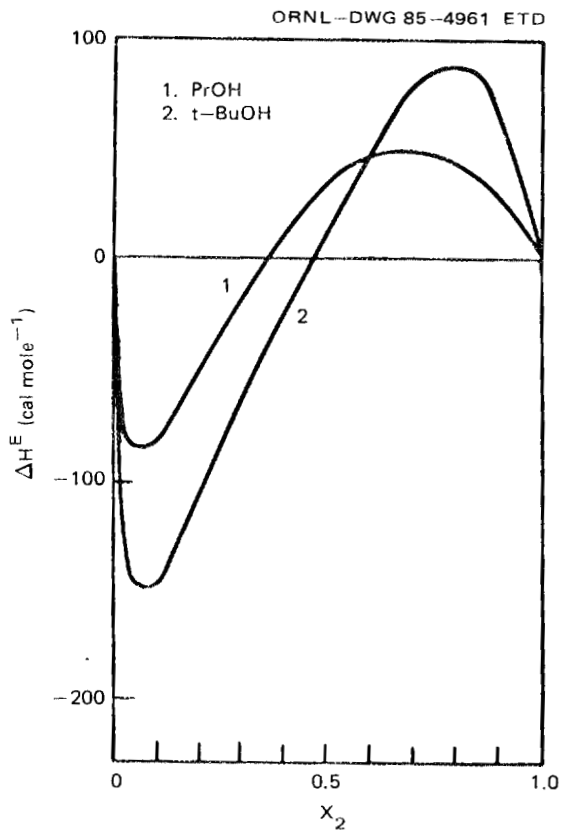

Fig. 13. Excess enthalpies of mixing of alcohols and water at 25°C. *Source*: F. Franks, *Physico-Chemical Processes in Mixed Aqueous Solvents*, American Elsevier Publishing Company, Inc., New York, 1967.

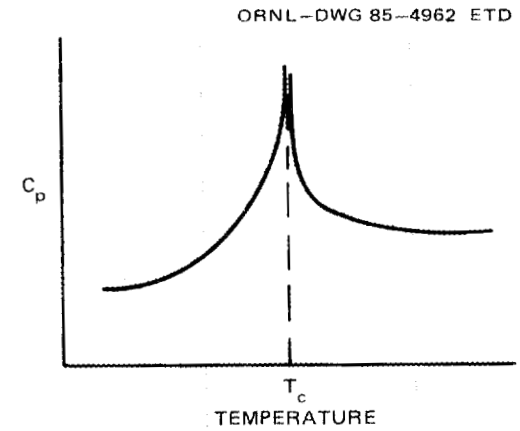

Fig. 14. Generalized C_p vs T curves for a CB.

theoretical point of view, the form of the curve is said to be the same as for a liquid-vapor critical transformation. The peak in the liquid-vapor case extends to infinity. Experimentally determined C_p curves for CBs generally show (Fig. 15) a merged or indefinite line at T_c.

To obtain the total heat stored over the temperature interval, therefore, the following procedure is called for:

$$\Delta H_{stored} = \int_{T_1}^{T_c} C_p \, dT + \int_{T_c}^{T_2} C_p \, dT + \Delta \, . \tag{2}$$

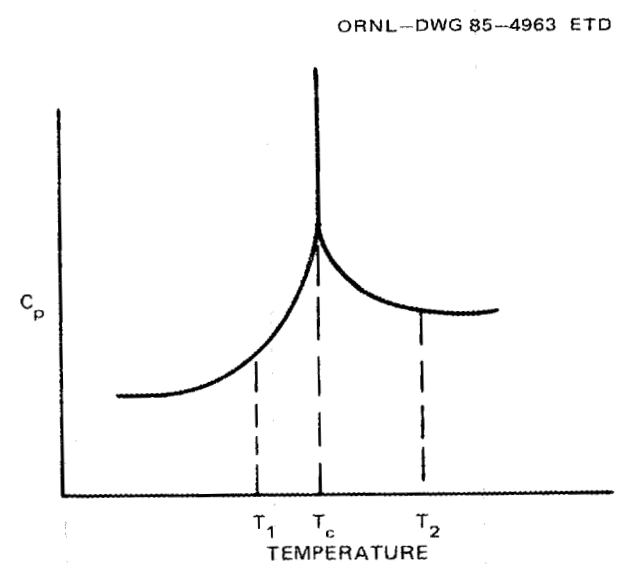

Fig. 15. Experimental C_p vs T curves for a CB.

The Δ term represents a latent heat, that is, a heat stored or liberated at the constant temperatures near the T_c. The literature is very uninformative about likely magnitudes of latent heats associated with CB phase transformations. CB systems with phase diagrams of Type 1 (Fig. 12), however, would be expected to have a higher latent heat than those of Type 2 because of the obvious greater extent of mixing or unmixing near the CST in the case of Type 1 systems.

2.1.3.1 Clathrate CB systems. Water and tetrahydrofuran (THF) form a clathrate hydrate, THF•17 H_2O, which has a Q_2 invariant temperature of 4.4°C at ~1 atm (Ref. 8). The Q_2 invariant temperature is the temperature where solid clathrate, two immiscible liquid phases, and one gaseous phase coexist in equilibrium. The enthalpy change for the reaction

Hydrate → Liquid 1 + Liquid 2

is reported as 19.5 kcal/mol (215.8 J/g) (Ref. 9).

The conjugating behavior of the water plus THF system is shown in Fig. 16 at a pressure slightly above atmospheric. The increased pressure

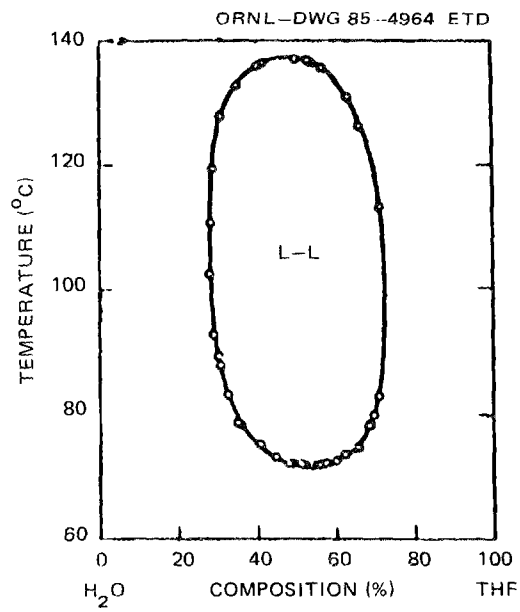

Fig. 16. Phase diagram for water and tetrahydrofuran. *Source*: D. W. Davidson, "Clathrate Hydrates," pp. 115–234 in *Water: A Comprehensive Treatise*, Vol. 2, Plenum Press, New York, 1973.

is required because the temperature region of immiscibility is above the boiling temperatures of the water/THF mixtures.

The heat of mixing characteristic of the water/THF system in the immiscibility region is not known but is probably on the order of ~20 J/g. At 25°C the heat of mixing is ~28 J/g (Ref. 10).

The CB characteristics of the water/THF system appear marginal for practical applications because the lower CST is somewhat too high (~71°C) and the heat of mixing not very high. However, the addition of a suitable third liquid to the system may overcome the weaknesses of the system.

Water plus sulfur dioxide (SO_2) forms a clathrate hydrate with a Q_2 temperature of 12.1°C at a pressure of 2.33 atm (Ref. 11). At a pressure of 1 atm, the decomposition temperature of the gas hydrate is 6.8°C. The system also exhibits CB behavior, as shown by the phase diagram in Fig. 17. The formation of the hydrate from two immiscible liquids is closely akin to the formation of a solid, pure component and a liquid from two immiscible liquids (monotectic phase change) discussed in Sect. 2.1.3.2.

Heats of clathrate hydrate formation and critical mixing have not been located. These are expected to be large, however, because sulfur dioxide has a large dipole moment (1.61 debye). The CST of about 130°C is too high, as is the required pressure of 35 atm, for home heating applications. For commercial applications, however, the given temperature and pressure characteristics of CB behavior might prove very acceptable for certain cases.

2.1.3.2 Monotectic CB systems. Systems that exhibit CB behavior often also show monotectic solidification. A generalized phase diagram for this type of system is shown in Fig. 18.

Cooling such a system at a constant rate from a single-liquid phase state (at a composition of 50% A + 50% B) would give a temperature-time curve along the lines shown in Fig. 19.

The change in slope of the curves at the indicated points show the onset of the specific phase changes. The dotted straight line indicates the temperature drop if no phase changes occurred. The monotectic phase change would generally be expected to be capable of storing a substantially greater amount of heat than the CB phase transition.

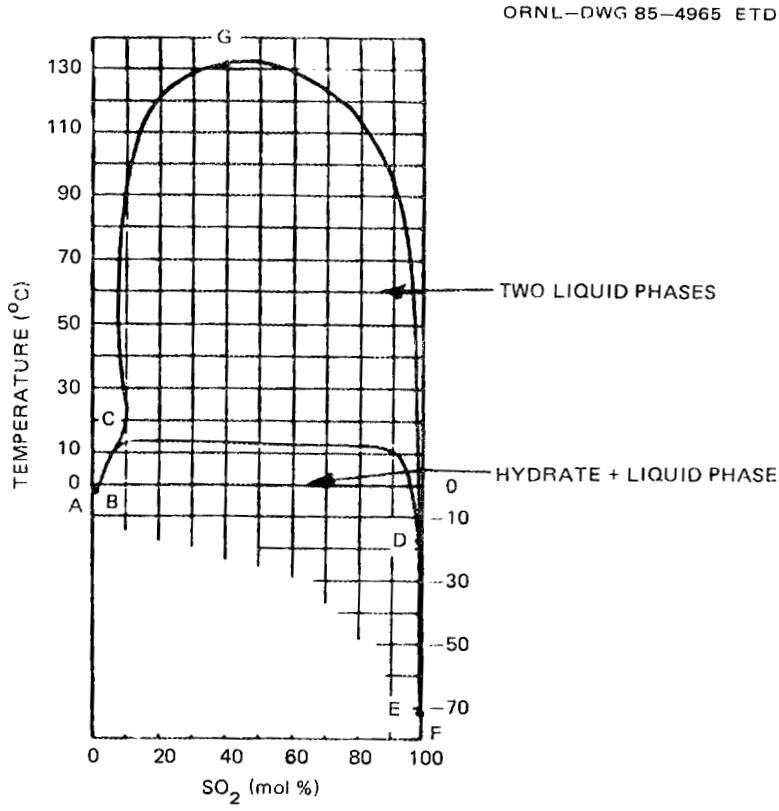

Fig. 17. Phase diagram of the water plus SO_2 system. *Source*: E. Terres and I. G. Ruhl, "Untersuchungen uber das binary System Schwefeldioxyd-Wasser. Zwei Modifikationen des festen SO_2," *Angew. Chem.* 47 (1934).

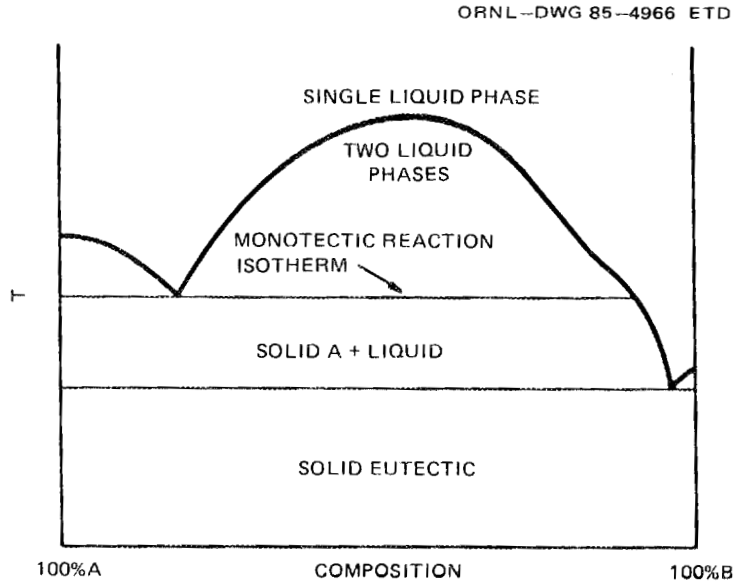

Fig. 18. Typical phase diagram for a monotectic CB.

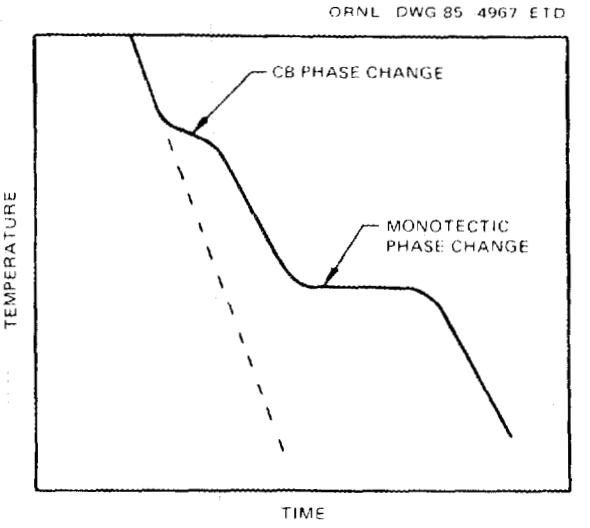

Fig. 19. Representative cooling curve for a monotectic CB.

One system that appears promising for dual-temperature storage consists of propylene carbonate and water (phase diagram shown in Fig. 20).

Heats of mixing data for the system were not found, but they are expected to be substantial. Ethylene carbonate has a heat of mixing with water of 145 J/g at 25°C.[10]

2.1.3.3 Closed-loop CBs. In this category, none of the systems reviewed had lower and upper temperatures in the right range. Also, the materials involved generally were fairly exotic and, thus, unlikely to qualify for practical CB systems on the basis of either cost, stability, or nontoxicity.

2.1.3.4 Higher pressure CB systems. The recent interest in supercritical fluids for extraction purposes raises the question of whether unique, practical CB systems might exist in which one or both of the fluids are either a condensed gas (liquid) or a supercritical fluid. A review of the literature revealed that the following types of CB systems are possible:

$$L_1 + L_2 \rightleftarrows L_s \text{ or } SCF_s ,$$

$$L_1 + SCF_2 \rightleftarrows L_s \text{ or } SCF_s ,$$

$$SCF_1 + SCF_2 \rightleftarrows SCF_s ,$$

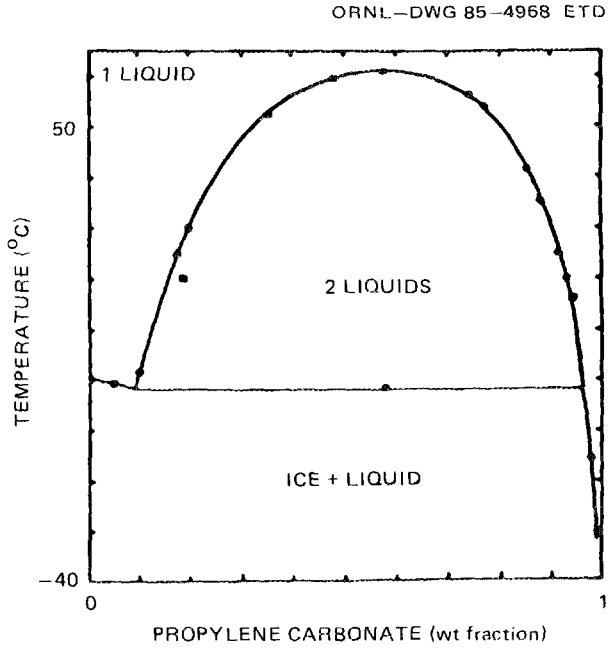

Fig. 20. Phase diagram for propylene carbonate-water. *Source*: N. F. Catherall and A. G. Williamson, "Mutual Solubilities of Propylene Carbonate and Water," *J. Chem. Eng. Data* 16 (1971).

where L stands for liquid phase, SCF for supercritical fluid, and the subscripts 1, 2, and s for, respectively, component 1, component 2, and solution. In the cases of liquid mixing with supercritical fluid or the mixing of two supercritical fluids, the critical temperatures are not called CSTs but just critical temperatures (CTs). Some of the common fluids that might be considered of interest in this area are shown in Table 1.

Most of the data found in this area are of no interest to the present study. The systems reported have been, for the most part, those of theoretical interest and those of interest to the petroleum industry. The pressures are, thus, too high or the heats of mixing too low for present purposes. For example, propane and methanol (50 wt % of each) have a heat of mixing of 9.7 J/g at 298.15 K and 2985 kPa (30 atm, 433 psi) (Ref. 12).

2.1.3.5 High-temperature CBs. Material categories for high temperature storage generally include the combinations metal plus molten salt plus salt. The category of molten oxides, silicates, phosphates,

Table 1. Some common fluid candidates for higher pressure CBs

Material	Melting point (°C)	Boiling point (°C)	Critical pressure (atm)	Critical temperature (°C)
Carbon dioxide	−78.5	−78.56	72.9	31.3
Sulfur hexafluoride	−56.0	−63.8	37.1	45.6
Ethane	−172.0	−88.28	48.3	32.9
Propane	−189.89	−44.50	42.0	96.8
Sulfur dioxide	−75.46	−10.02	78.1	157.6
Ammonia	−77.74	−33.35	112.3	133.0
Freon (CCl_2F_2)	−155.0	−30.0	39.56	111.5
Ethanol	−115.0	78.32	63.0	243.0
Water	0.0	100.0	218.3	374.2
Butane	−0.33	−0.6	37.47	152.0
Isobutane	−145.0	−12.2	36.5	133.7

etc., appears unpromising because of high viscosities and slow phase change kinetics. The desirability of keeping the molecular weights of the constituents of a CB as low as possible to maximize the heat of mixing necessarily restricts candidate materials in this area to alkali, alkaline earth metals, and their molten salts.

Most systems that appear at all practical display monotectic, as well as CB, phase change. Such systems should be able to store much more heat than molten salt systems that store heat only by means of sensible heat. In addition, high-temperature monotectic CB systems can offer an advantage over PCM systems because they can be designed to avoid crystallization on heat transfer surfaces, a major problem in PCM systems.

In summary, CB systems displaying the type of behavior depicted in the following equations appear most likely to be adaptable to practical dual-temperature storage systems for applications such as building heating and cooling.

Hill-type CB behavior at higher temperature, that is,

$$\text{Liquid 1} + \text{Liquid 2} \underset{-q}{\overset{+q}{\rightleftarrows}} \text{Clathrate} + \text{Liquid} ,$$

or

$$\text{Liquid 1} + \text{Liquid 2} \underset{+q}{\overset{-q}{\rightleftarrows}} \text{Solid 1} + \text{Liquid 2} ,$$

where +q indicates heating and −q, cooling.

For lower temperature ranges the system's propylene carbonate plus water (upper CST ~60°C, monotectic temperature approximately −5°C) and sulfur dioxide and water (upper CST ~130°C and clathrate temperature ~10°C) may eventually find applications in home or commercial heating and cooling.

For high-temperature applications the CB-monotectic system sodium-sodium chloride (Na-NaCl) appears promising.

Closed-loop CB material systems appear to have too wide a temperature interval between the upper and lower critical temperatures to be of much value for most practical dual-temperature storage applications. Also, the materials involved are generally complex, expensive, and toxic.

Data on CB systems of liquid or supercritical gases are so scarce that a definite conclusion on feasibility for TES cannot be reached at this time. The data found, however, indicate interesting possibilities with either liquid or supercritical polar gases and some hydrocarbons, although containment at pressures greater than critical may be expensive.

Preliminary economic analyses indicate that

1. CB-clathrate/monotectic systems are promising for load-leveling applications. A payback period of 9.3 years is calculated for a representative, dual-temperature CB-clathrate/monotectic system coupled to a 3-ton heat pump.
2. The CB-monotectic system sodium-sodium chloride (Na-NaCl) compares favorably with a high-temperature storage system based on sensible heat storage (sodium hydroxide) and latent heat of fusion storage (PCM pellet-packed bed).

It is expected that the enhanced heat transfer rates that are realizable with CB-clathrate/monotectic systems because of avoidance of crystal growth on heat transfer surfaces during the clathrate/monotectic phase change and because of the total liquid nature of the CB phase transition should considerably improve these preliminary economic projections.

2.1.4 Liquid and solid solutions (Project 1.3.4)

The propylene carbonate-water system was identified as having properties matching the requirements of dual-temperature storage, that is, storage at two temperatures appropriate for both the winter and summer seasons. Data for the heat of mixing of the system were not available for the applicable temperature range. Therefore, values of heats of mixing were estimated for propylene carbonate-water mixtures in the two liquid phase regions for temperatures to the upper critical solution point (T_{cs}). Mutual liquid-liquid solubility data for the system were presented by Catherall and Williamson[13] and by Hong et al.[14] The data from the two sources are not in agreement, with T_{cs} reported as 61.1°C in Ref. 13 and 71°C in Ref. 14. The values from the more recent reference (14) shown in Fig. 21 are considered to be more reliable, but there is some uncertainty concerning the correct data.

The Van Laar equations were utilized to represent the composition and temperature variation of the activity coefficients of the components for this system. For this model,

$$\ln \gamma_1 = \frac{A_{12}}{\left(1 + \frac{A_{12}}{A_{21}} \frac{x_1}{x_2}\right)^2} , \tag{3}$$

$$\ln \gamma_2 = \frac{A_{21}}{\left(1 + \frac{A_{21}}{A_{12}} \frac{x_2}{x_1}\right)^2} . \tag{4}$$

For liquid-liquid equilibrium,

$$\gamma_1^1 \, x_1^1 = \gamma_1^2 \, x_1^2 , \tag{5}$$

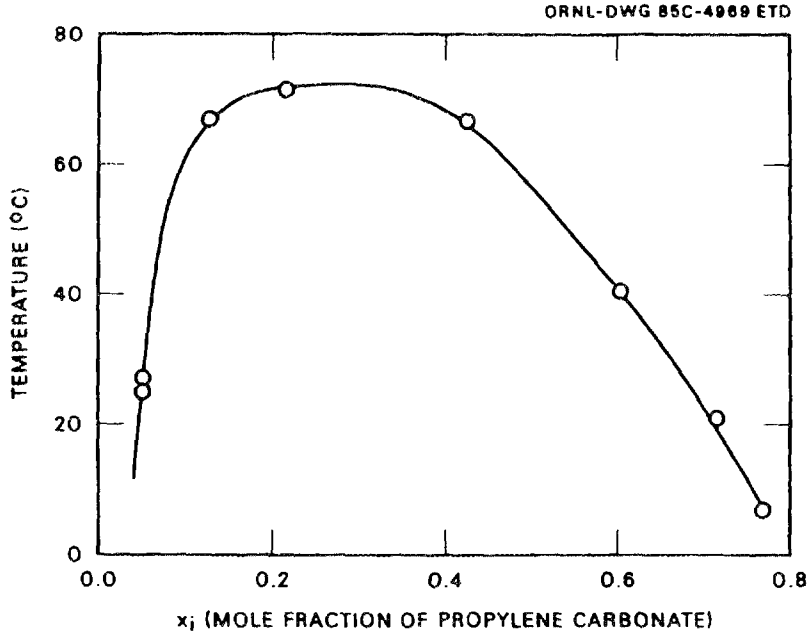

Fig. 21. Propylene carbonate-water material solubility.

$$\gamma_2^1 \, x_2^1 = \gamma_2^2 \, x_2^2 \, , \tag{6}$$

where x_1^1 and x_1^2 are the mole fraction of propylene carbonate in liquid phases 1 and 2, respectively.

The liquid-liquid phase data of Hong et al.[14] were used to solve for values of A_{12} and A_{21} for temperatures from 30 to 71°C. The resulting values of A_{12} and A_{21} vary linearly with 1/T except for A_{12} in the vicinity of T_{cs}, as shown in Figs. 22 and 23.

The heat of mixing is determined from the temperature variations of the activity coefficients as

$$\frac{\Delta H_M}{R} = x_1 \left. \frac{\partial \ln \gamma_1}{\partial (1/T)} \right|_{x_1} + x_2 \left. \frac{\partial \ln \gamma_2}{\partial (1/T)} \right|_{x_1} , \tag{7}$$

where R is the gas constant.

Values of ΔH_M at an overall composition $x_1 = 0.2$ (close to the critical composition) are presented below for temperatures between 30 and 71°C. At $T_{cs} = 71$°C, a value of $\Delta H_M = 33.7$ Btu/lb is calculated. The

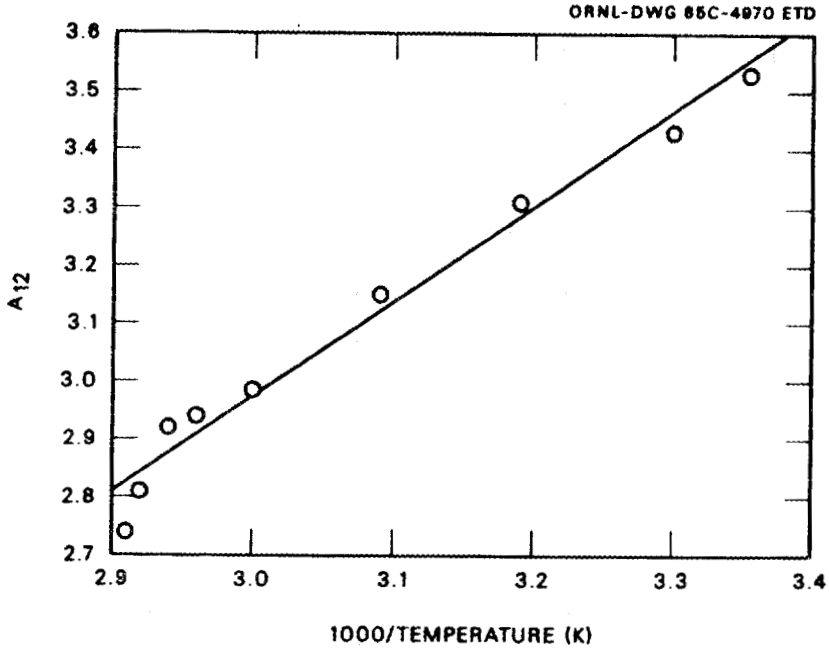

Fig. 22. A_{12} vs 1000/T°K, 25 to 71°C.

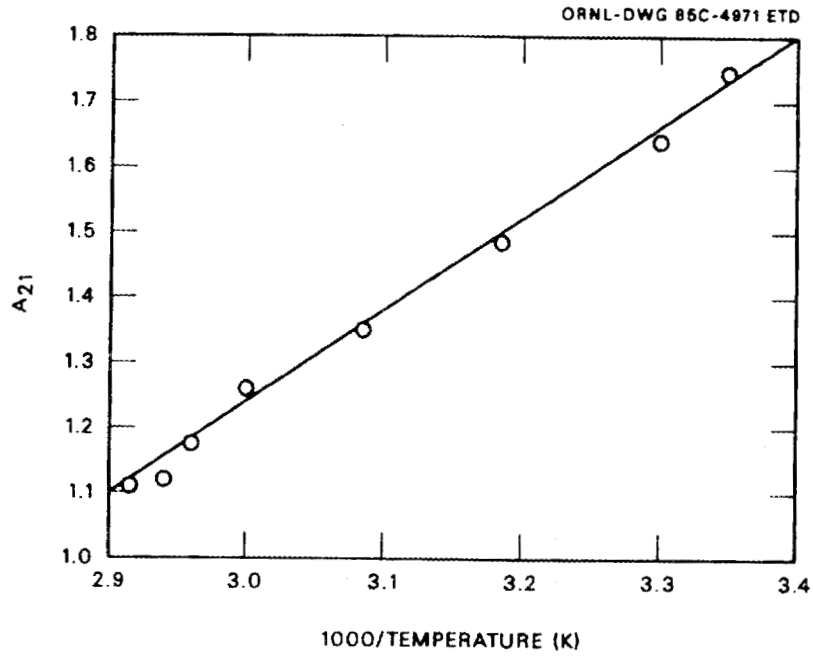

Fig. 23. A_{21} vs 1000/T°K, 25 to 72°C.

corresponding differences in the heat of mixing at T_{cs} and at lower temperatures in the two liquid phase regions range from 9.5 Btu/lb at 60°C to 22.8 Btu/lb at 30°C. This difference would represent the heat recovered on cooling the mixture to the lower temperature and would be in addition to the sensible heat gain ΔH_s. The following applies, assuming a heat capacity of 0.5 Btu/lb°F for propylene carbonate:

T_2 (°C)[a]	x_1^1	x_1^2	ΔH_M^1	ΔH_M^2	$\Delta H_M\|_{T_2}$	$\Delta H_M\|_{T_1} - \Delta H_M\|_{T_2}$
60	0.088	0.435	22.15	28.5	24.2	9.5
50	0.065	0.521	16.5	23.9	18.8	14.9
40	0.051	0.599	12.3	19.7	14.4	19.3
30	0.042	0.666	9.1	16.1	10.9	22.8

[a] T_1 = 71°C; x_1 = 0.2; ΔH_M = 33.7 Btu/lb.

The analysis, however, indicates that ΔH_M at T_{cs} could be as high as 36 to 40 Btu/lb, which would increase the differences in heats of mixing presented in Table 1 by 2 to 6 Btu/lb.

The indicated behavior in the critical region appears to reflect an increase in the heat capacity of the mixture at these conditions. The heat capacity is related to the enthalpy of the mixture as follows:

$$C_{pM} = \left(\frac{\partial H_M}{\partial T}\right)_p . \tag{8}$$

Hildebrand and co-workers[15,16] measured heat capacities in the critical region for several mixtures with upper and lower critical solution temperatures. A sharp increase in the heat capacity at T_{cs}, which persists for higher temperatures, was indicated. More recent experiments[17,18] exhibited a smaller increase in C_{pM} for a narrower temperature range in the critical region. In the latter studies, the heat capacity at the critical composition was represented as

$$C_{pM} = D + E\,\varepsilon^{-\alpha} , \tag{9}$$

where D and E are constants, $\varepsilon = (T - T_{cs})/T_{cs}$, and $0.1 < \alpha < 0.2$. Since phase equilibrium data are not available for propylene carbonate/water mixtures for temperatures above T_{cs}, heats of mixing at higher temperatures could not be estimated for this system.

A literature search was conducted for phase equilibria data for the ethylene carbonate/water system. Carbon et al.[19] determined several properties for this system at 40°C, including dielectric constants, viscosities, and densities. This system was reported to be completely miscible at 40°C and partially miscible at room temperature. The data were found to indicate an increase in complexity of the system at high concentrations of ethylene carbonate. Cunningham et al.[20] determined physical properties for this system at 25°C and freezing point data (solubility limits) for −2 to 36°C, the freezing point of ethylene carbonate. Lakhanpal et al.[21] determined the solubility limit, equilibrium pressures, and heats of solution for this system.

Zakirov[22] measured densities and boiling points of solutions of ethylene carbonate and water at 25 and 40°C. The results suggested that unstable hydrates were formed at high concentrations of ethylene carbonate. Geller[23] also suggested the formation of hydrates for this system at 50°C, based on the behavior of his data for specific heats and heats of solution.

In Fig. 24 values of the solubility limits for this system from the data of Cunningham et al.[20] are shown. This information was used in conjunction with the data for heats of solution presented by Lakhanpal et al.[21] to estimate cool storage capabilities for this system. The initial condition was a saturated solution at 15°C (weight fraction of ethylene carbonate = 0.27) that is cooled to −2°C (weight fraction of ethylene carbonate = 0.1). The heats of mixing values presented by Lakhanpal et al.[21] were corrected to account for the heat of melting of the solid component in the solution. The calculations indicate a storage capacity of about 42 Btu/lb of initial solution, compared to 31 Btu/lb for the sensible heat of water. This value does not include any contribution from the formation of ice. It can be seen from Fig. 24 that this system could provide effective heat storage capabilities only at a high

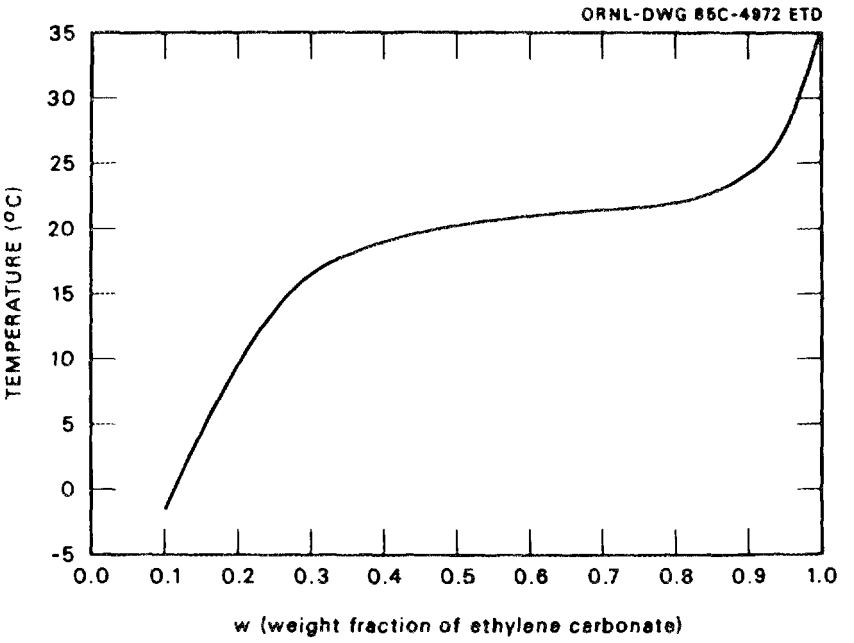

Fig. 24. Solubility limits, ethylene carbonate-water.

concentration of ethylene carbonate. For a combined heat and cool storage system, the liquid phase at the lowest temperature in the cooling mode would have to be separated from the solid phase before use in the heating mode.

2.2 TES Media Development

Several storage materials have survived the investigative assessment stage and remain as viable candidates for development. Projects in this category are aimed at defining the performance of TES media in a specific storage system application. Three such projects were pursued during the reporting period. Two are in the high-temperature, industrial waste heat recovery area where major conservation gains are to be possible. The third project addresses the cool storage requirement found in much of the summer air-conditioning regions of the United States.

2.2.1 Gas clathrates for heat pump cool storage (Project 2.1.1)

Several heat pump refrigerants form gas hydrates (clathrates) that have good potential as cool storage media for heat pump systems.[24-26]

These icelike materials have several characteristics that give them an advantage over chilled water or ice storage. Like ice, a clathrate stores energy as latent heat, thereby giving it an advantage of lower storage volume over sensible heat storage in chilled water. Latent heat storage also presents a much reduced temperature range to the evaporator coil. Additionally, fluorocarbon clathrates freeze at higher temperatures (10 to 12°C) than ice, providing an advantage in heat pump capacity over that achieved when freezing ice for storage. These advantages may be amplified by the possibility of direct contact heat transfer into and out of storage because the fluorocarbon is both the refrigerant and, with water, the storage medium. Thus, the heat-transfer penalty from heat exchanger surface temperature drops may be avoided. Finally, storage at higher than ice temperature can reduce heat gain of the storage vessel.

The phase diagram for R-12/H_2O mixtures is shown in Fig. 25. R-12, like many refrigerants, is only slightly soluble in water; thus, curve A-Q_2-D very closely approximates the vapor pressure curve of R-12 alone.

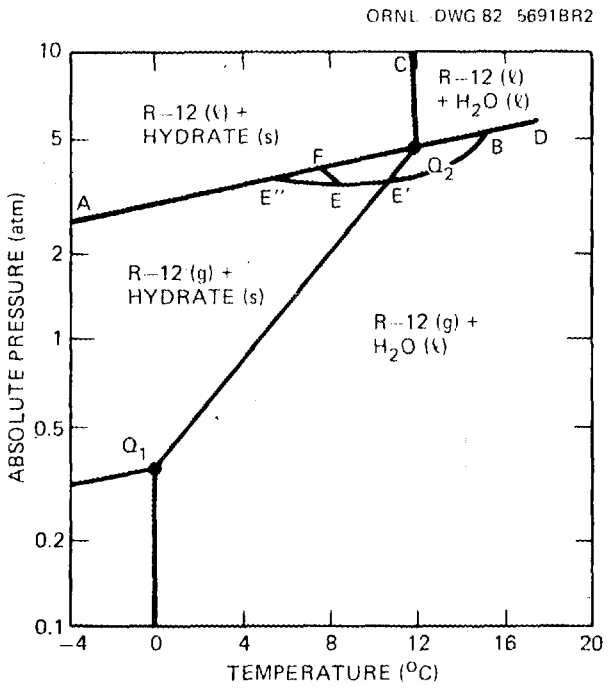

Fig. 25. Phase diagram for R-12/H_2O mixtures.

Points Q_1 and Q_2 are invariant quadruple points where four phase equilibria exist, and the line Q_1-Q_2 defines a transition from $H_2O(\ell)$ and R-12(g) to the R-12 gas hydrate, releasing a heat of formation of 76 kcal/kg of hydrate.

A conceptual cool storage system based on the R-12 gas hydrate is shown in Fig. 26. The system consists of a vapor-compression refrigeration cycle with the conventional evaporator replaced by a storage tank crystallizer in which the gas hydrate is formed and dissolved. A completely discharged storage tank consists of R-12(g), R-12(ℓ), and $H_2O(\ell)$ in equilibrium, as shown at point B in Fig. 25. At the initiation of the charging period, the compressor will reduce the pressure in the storage tank, causing R-12(ℓ) to vaporize. This, in turn, reduces the temperature in the storage tank. The pressure and temperature will continue to decrease in such a manner until Q_1-Q_2 curve is crossed and gas hydrate begins to form. The heat released by the formation of the gas hydrate vaporizes the R-12(ℓ). When the rate at which R-12(g) produced in this manner is sufficient to maintain a constant pressure in the storage tank, an equilibrium (point E) will be reached. The position of point E depends on the thermal driving force required to produce the gas hydrate ($T_{E'} - T_{E''}$) . Gas hydrate continues to form until all the $H_2O(\ell)$ in the

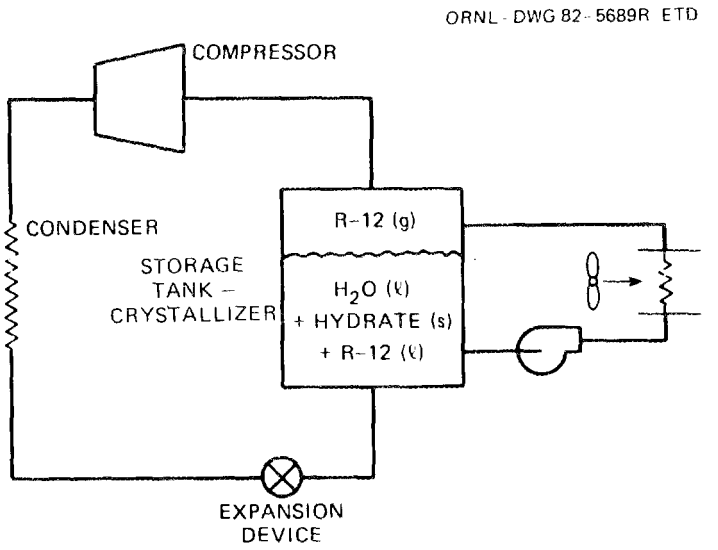

Fig. 26. Conceptual gas hydrate cool storage system.

storage tank is consumed, at which time the charging process is complete. The completely charged storage tank will consist of R-12(g), R-12(ℓ), and R-12 gas hydrate in equilibrium, as shown at point F. A small amount of R-12(ℓ) should remain in the storage tank to be used later to initiate discharge of the storage system via a pump, fan, and evaporator coil in the building supply duct.

Experiments to study the gas hydrate formation process were completed in the preceding year.[27,28] These experiments were conducted in a manner that simulated the operation of a proposed storage system that uses a gas hydrate as the PCM. Accordingly, they verified the formation of gas hydrate under appropriate pressure and temperature conditions; defined the thermodynamic conditions under which the system operates to form a gas hydrate; characterized the performance of the hydrate formation process as a function of several parameters; and using direct-contact, heat-exchange methodology, ascertained the discharge capacity of the storage system.

This year's investigation was of clathrates of mixed fluorocarbon refrigerants. The R-12/water phase diagram upper invariant point of 449 kPa requires a pressure vessel to contain the clathrate, an economically unattractive fact for commercialization.

The characteristics of three refrigerants — Trichloromonofluoromethane (R-11), Dichlorodifluoromethane (R-12), and Dichloromonofluoromethane (R-21) — that form clathrates at temperatures suitable for cool storage are shown in Table 2. These refrigerants combine with water to form a

Table 2. Characteristics of refrigerants considered in this study

Refrigerant	Q_2		Molecular weight	Water (mol)	Latent heat of fusion [J/g (Btu/lb)]
	Temperature [°C (°F)]	Pressure [kPa (psia)]			
R-11 (CCl_3F)	8.7 (47.6)	59 (8.6)	137	16.6	281.7 (121.2)
R-12 (CCl_2F_2)	12.1 (53.8)	449 (65.4)	121	15.6	270.4 (116.6)
R-21 ($CHCl_2F$)	8.6 (47.5)	101 (14.7)	103	16.9	276.6 (118.9)
R-114 ($C_2Cl_2F_4$)	No hydrate		171		

clathrate according to the reaction

$$R(\ell) + M \cdot H_2O(\ell) \rightarrow H(s) + h \ . \tag{10}$$

The number of molecules of water n needed to form the hydrate per molecule of each of these refrigerants is given in Table 2. Also shown are the heat of formation h per unit mass of the clathrate and the upper invariant point (Q_2) or pressure and temperature at which the clathrate forms.

Refrigerant R-21 forms a clathrate at atmospheric pressure; however, this refrigerant is very chemically active and would only be appropriate for a closed system, that is, separated from the heat pump refrigerant by a heat exchanger. Refrigerant R-11 forms a clathrate at <1 atm. The possibility of forming a clathrate at 1 atm by mixing R-12 and R-11 then exists.

When a single refrigerant such as R-12 is used in a gas hydrate, cool storage system, the gas hydrate is formed at point Q_2 of the phase diagram of the refrigerant/water system (Fig. 25). The pressure and temperature of this point correspond to that shown in Table 2. In a cool storage system, gas hydrate (solid) will coexist with some water (liquid), some refrigerant (liquid), and a gaseous portion containing the refrigerant saturated with water vapor. This system has two components (water and refrigerant) and four phases (liquid refrigerant, liquid water, solid hydrate, and vapor). According to the phase rule,[29]

$$F + P = C + 2 \ . \tag{11}$$

For the cool storage system with a single refrigerant, the phase rule yields

$$F = C + 2 - P = 2 + 2 - 4 = 0 \ . \tag{12}$$

Therefore, no degrees of freedom are available, and the system, when in equilibrium, has to operate at the invariant point Q_2 (Fig. 25), where R-12(ℓ), R-12(g), $H_2O(\ell)$, and gas hydrate can coexist.

If two completely miscible refrigerants are used to form a mixed clathrate, the situation changes. Now, the system has three components

(water and two refrigerants) but the same four phases as in the previous case. The degrees of freedom that are available now are

$$F = C + 2 - P = 3 + 2 - 4 = 1 \ . \tag{13}$$

One degree of freedom indicates that the pressure-temperature relationship for the mixed hydrate is uniquely dependent on the composition of the mixture of refrigerants. Mixed-hydrate formation should occur at a point between the two Q_2 points of the single refrigerants in the mixture, a fact confirmed by previous experiments.[30] If, however, only one refrigerant is used, the hydrate will form at the end of this line corresponding to the Q_2 point of the refrigerant used.

If a mixture of two refrigerants — one that does not form a hydrate [like Refrigerant-114 (R-114)] and the other one entering into the hydrate — is used, the same situation as the one given by Eq. (13) occurs. Still, three components and four phases will be present, and, therefore, one degree of freedom will be available. Hydrate will be formed at different pressures and temperatures, depending on the composition of the mixture, with only the hydrate-forming refrigerant entering into the hydrate. Inactive R-114 and the remaining water, if any, will not combine and will remain as liquid coexisting with the solid hydrate.

Mixtures of R-11 and R-12 were tested. The results are shown in Fig. 27, which is a phase diagram showing the locus of Q_2 points for various ratios of refrigerants. The mixture composition of 0.88 mole fraction of R-11 and 0.12 mole fraction of R-12 forms a mixed hydrate at 1-atm pressure and at 9.2°C (48.6°F).

Clathrates of mixtures of R-11 and R-14 (dichlorotetrafluoromethane) were also formed. Only R-12 entered into the clathrate. By varying the composition of the mixture, clathrates over a range of temperatures and pressures were obtained. All of the hydrates formed at pressures below atmospheric and temperatures below 8.7°C (47.6°F).

Finally, clathrates from mixtures of R-12 and R-114 were also produced. Only R-12 entered into the clathrate structure as in the case of R-11/R-114. For temperatures above 0°C (32°F), all of these clathrates were at pressures above atmospheric.

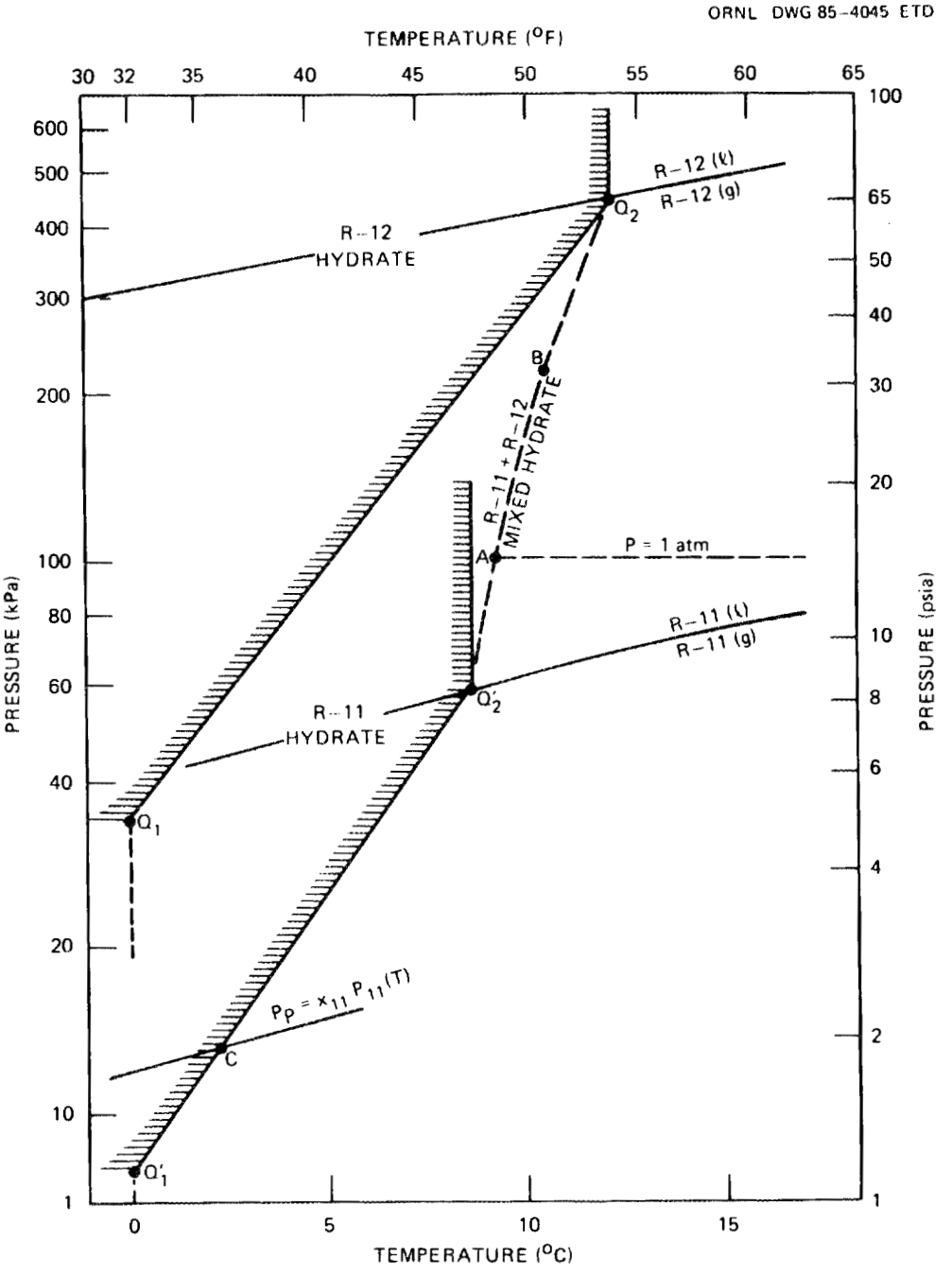

Fig. 27. Phase diagram for R-12 + R-11 + H_2O.

Tests to simulate heat pump storage were successfully completed in the experimental crystallizer. Mixtures of R-11/R-12 formed clathrates in the closed system, required because of the different vapor pressures of the two refrigerants, by cooling the refrigerant-water mixture. Discharge tests in which excess refrigerant was circulated through an external heat transfer loop were accomplished without problems.

2.2.2 Encapsulated metallic storage media (Project 2.5.1)

The goal of this research effort[31] is to develop the means of encapsulating metallic PCMs so that they can be used in direct-contact heat storage beds. The materials of primary interest are silicon-containing binary or ternary alloys, principally Al-Si and Al-Si-Mg alloys. Encapsulation techniques being investigated include surface treatments to achieve a pure silicon or an oxide shell and modified shotmaking techniques in an effort to achieve self-encapsulation with a pure silicon shell.

To see how self-encapsulation might be possible, consider the binary phase diagram of Fig. 28 for the Al-Si eutectic system, a promising, inexpensive medium for storage of heat at the eutectic temperature of 577°C. Consider the consequences of selecting a gross hypereutectic composition of 27 wt % Si, with a liquidus temperature of 800°C, and cooling such a liquid from 900°C by using jetting or shotmaking processes so that a spherical shot of perhaps 1-cm OD is produced. Shotmaking involves the controlled pouring of the liquid metal (perhaps through a screen) into a tall reservoir or a warm quench fluid, such as a fused salt, slag, oil, or organic liquid. The quench fluid and the other process variables are chosen such that surface tension forces stabilize a spherical droplet that is then solidified as shot of the desired size.

Upon the controlled cooling of the Al-Si alloy from 900°C in the shotmaking reservoir, first a solid of nearly pure silicon should begin to form at 800°C as a spherical shell in contact with the quench medium. As heat is further withdrawn from the sphere around the liquid core, the crust of nearly pure solid silicon would thicken. Finally, according to a quasi-equilibrium freezing process, at 577°C the liquid core with the

ORNL-DWG 85-4973 ETD

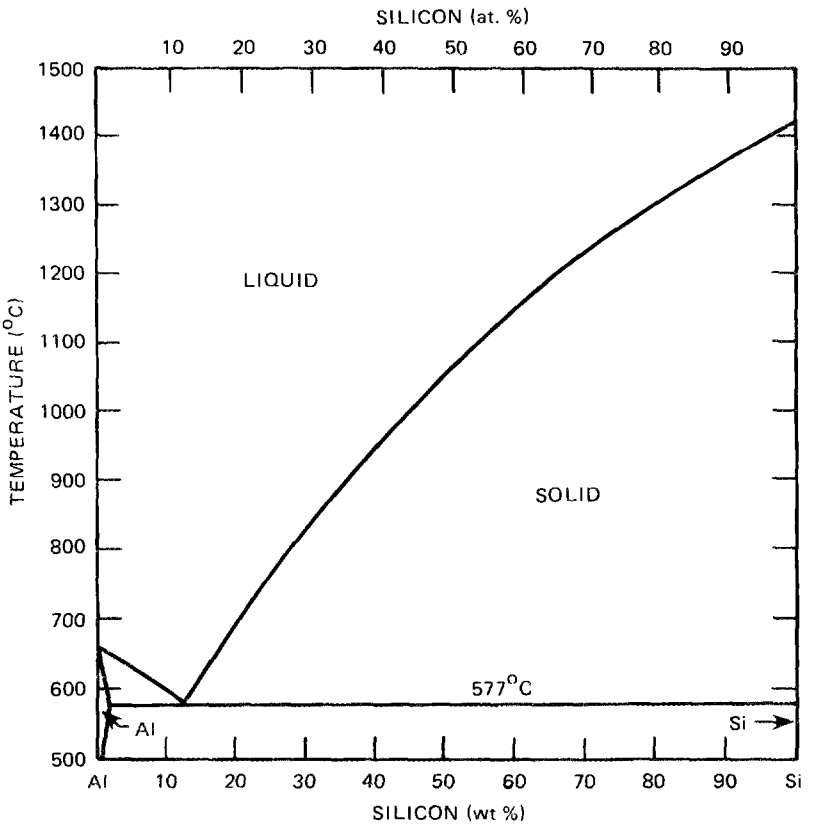

Fig. 28. Binary Al-Si phase diagram.

eutectic composition within the solid silicon case would solidify isothermally and release a large latent heat of solidification. For the specific Al-27 Si composition chosen for this example, the lever law indicates that a solid silicon shell would form, accounting for 16.5 wt % of the shot with the balance being 83.5 wt % for the eutectic core. With the use of room-temperature densities for silicon and aluminum (as the first approximation), these proportions correspond to a silicon shell of 6.6% of the shot radius (regardless of the actual radius) and 93.4% of the shot radius for the eutectic core. Obviously, these proportions are readily changed in a predictable manner by choosing a different gross composition for the shot.

The research work during this reporting period focused on three areas: encapsulating techniques, thermal and physical properties measurements, and performance modeling of a TES unit using the encapsulated media.

Several encapsulating techniques were investigated, including both self-encapsulating and surface modification modes. Experiments were performed to ascertain the feasibility of obtaining an integral silicon shell, as well as the conditions necessary to do so. In preliminary experiments, small amounts (e.g., 150 g) of salt mixtures were melted in iron crucibles, and the temperature of the fused salt was stabilized at 600, 650, 700, or 750°C. Al-30% Si alloys were melted, and a small quantity of the alloy was poured into the salt melts. The solidified Al-Si alloy samples were then removed from the cooled system and examined. Based on these screening trials it was found that

1. all of the shot produced had spherical or near spherical form,
2. none of the shot exhibited an integral outer silicon shell, and
3. all produced shot exhibited large primary silicon platelets at the surface and in the interior.

Following these preliminary results, additional experiments were conducted to screen and select appropriate salts to increase the nucleation density for the primary silicon at the surface of the shot. During this set of experiments, different combinations and proportions of fused salts — such as NaCl (sodium chloride), $AlCl_3$ (aluminum chloride), KCl (potassium chloride), $CaCl_2$ (calcium chloride), $Na_4P_2O_7 \cdot 10H_2O$ (sodium pyrophosphate), Na_2SO_4 (sodium sulfate), and $NaAlF_4$ (cryolite) — were examined. In these experiments a small quantity of Al-30% Si alloy was placed in an alumina crucible and then covered with the appropriate salt and the contents melted at 900°C for 45 min. Some samples were allowed to solidify inside the furnace at a low cooling rate (2.2°C/min), while others were cooled outside the furnace at a high cooling rate (1°C/s). The morphology of the primary silicon phase on the surface of the shot varied from large platelets to rounded modules, depending on the salt composition. The size and fraction of surface coverage by the primary silicon was quench-rate dependent, with finer primary silicon and greater surface

coverage occurring with increasing cooling rate during solidification. From these experiments it was concluded that NaCl was the best alternative to Kolene Salt for improving the nucleation of primary silicon on the surface of the Al-Si shot. However, the silicon surface coverage was typically between 40 to 70% and never exceeded 90%.

Based on the modification by phosphorus of Al-Si alloys, a new set of experiments was performed using Al-30% Si alloy containing 0.11% P. The salts used were NaCl and KCl. These experiments generated both smaller primary silicon crystals at the surface of the shot and, compared to the previous shot made without phosphorus, a better distribution of primary silicon crystals in the structure of the shot.

An experimental-scale shot tower (see Fig. 29) was designed and constructed. The 6-in.-ID steel pipe is 6 ft tall and is filled with the salt quenchant. Heat for the tower is supplied by four box heating units, each containing nichrome resistance heating wire rated at 5000 W. The tower is capable of maintaining a temperature gradient of 42°C/ft. Once the salt selection has been made, the shot tower will be used to verify that the self-encapsulated shot can be produced in a commercial facility.

Experiments in which the Al-30% Si alloy was melted, slowly cooled, and held for 10 min at a temperature 10° below the alloy liquidus temperature in a fused silicon tube produced silicon-encapsulated pellets. The shell of primary silicon was relatively uniform with a thickness between 0.06 and 0.08 mm. Based on the inverse lever rule, this shell thickness is consistent with the predicted equilibrium shell thickness. The silicon layer that formed in these experiments results primarily from the displacement reaction between liquid aluminum and silica:

$$4Al(\ell) + 3SiO_2(s) = 2Al_2O_3(s) + 3Si(s) \ . \qquad (14)$$

To better control and utilize this approach for the production of silicon-encased Al-Si alloys, a series of experiments are under way to evaluate the kinetics of the reaction.

Also evaluated were techniques in which pellets with an incomplete silicon shell as a result of the solidification process could be further

ORNL-DWG 85-4974 ETD

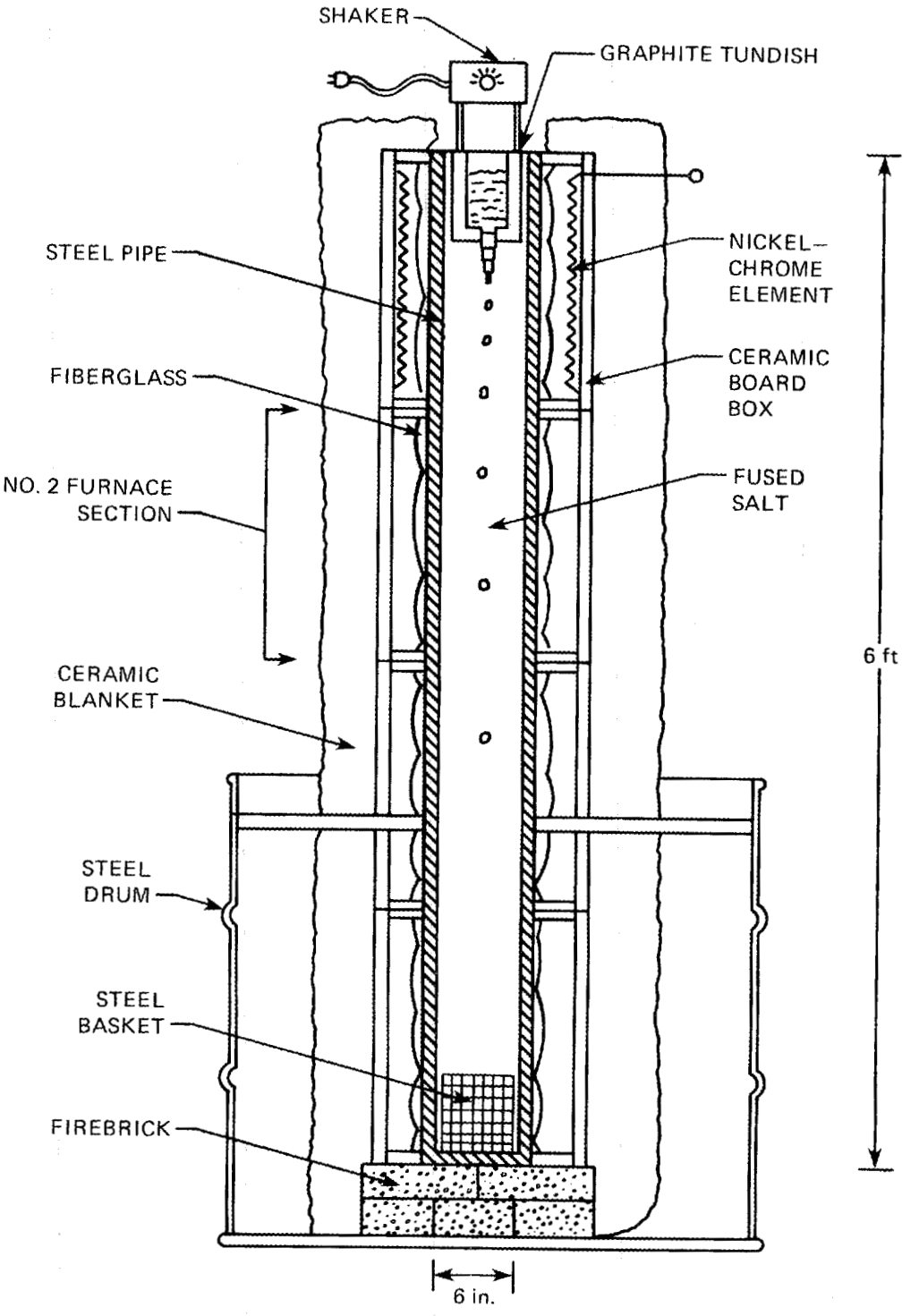

Fig. 29. Pilot shot tower.

treated to obtain the desired encapsulation. Using a pack cementation siliconizing process, experiments were conducted to produce silicon-encased Al-Si alloy shot. In this process the Al-Si shot is thermally treated in a halide-activated bed of silicon. These experiments indicated that using silicon as the pack matrix materials was preferable to using alumina. Specifically, the pack had the following composition: 73% SiO_2, 25% Si, and 2% activator (NH_4Cl and $AlCl_3$ in a ratio of 2:1). The pack was protected by N_2-5% H_2 gas. The Al-Si samples were treated at 600°C for 8 h and air-cooled. Integral silicon shells were obtained.

Evaluation of thermal properties of the heat storage shot has been performed using Differential Thermal Analysis (DTA)/Differential Scanning Calorimetry (DSC) and thermal cycling tests. The DTA/DSC analyses are being carried out using a Perkin-Elmer DTA 1700 System. The DTA/DSC unit has been calibrated using the enthalpy of fusion of pure aluminum. The enthalpies and temperatures of transformation for various Al-Si alloys have been measured. Using scan rates between 0.5 and 20°C/min, DSC runs were conducted in the temperature range of 500 to 800°C on selected samples of the Al-30% Si alloy. The results of the DSC experiments on the Al-30% Si alloy are summarized in Table 3. The values obtained using the slowest scan rate (0.5°C/min) are assumed to be the most representative of the sample because undercooling may occur during the cooling cycle. Thus, the heat of transformation for the Al-30% Si alloy without the phosphorus addition is 79.8 cal/g.

An apparatus designed for the thermal cycling of Al-Si shot consists of two tungsten-filament quartz lamps, each operating at 110 V, 10 A, connected to a timer and temperature controller. The shot is held by a thermocouple (TC) and is positioned at the mutual focus between the lamps. During the heating cycle, the lamps heat the shot to the required temperature (650°C). Then the shot is maintained at 650°C during the period of the heating cycle (15 min) by the temperature controller. During the cooling cycle, the potentiometer supplies a voltage of 6.382 mV, which equals the difference in TC emfs between 650 and 500°C. Therefore, the temperature of the shot falls to 500°C and is maintained there by the temperature controller for the period of the cooling cycle (15 min).

Table 3. Thermal data for Al-30% Si alloy

Condition	Scan rate (°C/min)	Heat of transformation (cal/g)	Peak temperature (°C)
		Al-30% Si	
Heating	0.5	79.79	572.8
Cooling	−20.0	−71.90	540.5
		Al-30% Si +Cu-P	
Heating	0.5	81.89	570.7
Cooling	−0.5	−67.20	561.9
Heating	2.0	87.49	573.6
Cooling	−2.0	−82.39	559.7
Heating	20.0	73.11	589.2

In the initial thermal cycling tests, exudation of liquid from the shot core was observed. Using the Clausius equation, accurate determination indicated that the solidification shrinkage is 3.6%. The magnitude of this value explains why exudations appear. The Al-Si eutectic existing near the surface of the shot undergoes sufficient expansion to rupture the thin surface layer and causes an exudation. This problem will be eliminated when thicker, more uniform silicon surface layers are achieved.

To date, silicon-based binary alloys spanning the temperature range of 577 to 1400°C have been identified (see Table 4).

A computer model has been developed to model the thermal response for a packed bed filled with PCM shot. Results from this computer code have indicated that because of the high thermal conductivity of the shot, it is advantageous to charge and discharge the bed with flow in the same direction. This results in a relatively uniform bed temperature and a high bed utilization factor.

Table 4. Silicon eutectics for heat storage

Alloy	Eutectic melt temperature (°C)	Eutectic composition (% Si)	Calculated heat storage capacity (kJ/kg)
V-Si	1400	95	1921
Zr-Si	1363	75	1685
Ti-Si	1333	78	1570
Cr-Si	1323	75	1515
Mn-Si	1178	51	1090
Be-Si	1090	61	1812
Ca-Si	1023	61	1111
Ni-Si	960	38	609
Mg-Si	940	57	1212
Cu-Si	802	16	422
Al-Si	577	12	571

2.2.3 Composite high-temperature storage material (Project 2.6.1)

A high-temperature storage medium that allows the latent heat fusion of a eutectic salt (sodium/barium carbonate) to be utilized in a packed bed storage system is under development. The concept, which has been demonstrated in laboratory scale, immobilizes the molten salt in a solid ceramic (magnesium oxide) matrix. The resulting material can be formed into convenient-size pellets for use in a packed bed, thus allowing both efficient direct-contact heat exchange between the storage charge/discharge fluid and the use of nitrate salts without the need for containment of liquid in corrosion-resistant vessels. Direct-contact heat exchange is advantageous because of both increased efficiency and circumvention of the heat-exchanger encrustation problem that is inherent in liquid/solid storage media systems requiring heat exchangers.

There are many congruently melting carbonate salt mixtures that could be used for latent heat storage. The program has concentrated on the investigation of two: 47.8 Na_2CO_3-52.2 (wt %) $BaCO_3$ and Na_2CO_3, both combined with an MgO matrix. The Na_2CO_3-$BaCO_3$/MgO composite medium was selected for initial testing of this storage concept because of its good thermal stability and mechanical strength. The Na_2CO_3/MgO composite was

investigated because of the material low cost and high energy-storage capacity of Na_2CO_3.

Two deficiencies in the sodium carbonate composite remain to be overcome. As much as 6% weight loss in 400 h at a temperature of 900°C (Na_2CO_3 melts at 858°C) has been attributed to formation, and vaporization, of N_2OH and is unacceptably high. Secondly, excessive MgO particle growth at 900°C is observed. Attempts to stabilize the MgO particle size by the addition of $NaAlO_2$ were unsuccessful. For these reasons, further research on the sodium carbonate composite has been postponed in favor of completing the development and characterization of the sodium-barium carbonate composite medium.

Preliminary economic studies of the value of TES in the brick and tile industry yielded a maximum allowable installed cost of $24/kWh. An estimate of installed capital costs of systems utilizing the Na_2CO_3-$BaCO_3$/MgO medium yielded $19.78/kWh. This estimate was based upon a projected medium cost of $0.23/lb. In view of the small differences between allowable and estimated installed cost, effort was continued towards medium processing and fabrication costs.

Attempts to simplify the pellet processing and fabrication scheme by dry-blending the component powders and forming pellets directly from the powder blend were successful. It was observed that pellets pressed from dry blended powders were susceptible to cracking during heat treatments. It was further observed that the addition of binder solution to the powder resulted in relatively fewer cracks in the pellets. Apparently, water of the binder solution reacts with the powder and modifies the powder characteristics.

A procedure that produced crack-free sintered pellets has been established for dry-blended Na_2CO_3-$BaCO_3$/MgO powder mixture. This procedure involves adding sufficient water to the powder (1 part water to 2.5 parts powder by weight), drying at 150°C for 15 h, and die-pressing without additive at 5000 psi. The pellets are then sintered at 1100°C for 2 h to a density of 3.05 g/cm^3 or 90% of theoretical. This procedure will be used to manufacture the pellets required for the packed-bed stability test and the samples for thermal conductivity measurements and is expected to yield a processing cost less than $0.25/lb.

Additional thermal cycling tests of a 40-lb bed of sodium-barium composite pellets were conducted to investigate material physical and chemical stability. In over 6000 h of testing, 200 melt/freeze cycles were imposed. Results show an acceptable loss of carbonate from the bed (<1%). However, there is a migration and redistribution of carbonate within the bed, and the mechanism of these was investigated.

The most significant factor leading to salt migration appears to be vaporization of volatile components. If the support medium (MgO) is sufficiently filled with molten salt, under appropriate temperature/flow-rate conditions salt vaporization may occur at the medium surface. The more-volatile component vaporizes, leaving the less-volatile component on the surface as a solid residue. Na_2CO_3 is more volatile than $BaCO_3$. Thus, as vaporization continues, the local surface barium-to-sodium ratio would increase. The possible Na_2CO_3 transport mechanisms from the interior to the surface are viscous flow through the capillaries, vapor transport through interconnected pores, and ionic diffusion of Na^+ through the carbonate network.

If ionic diffusion and/or vapor transport are swift (i.e., controlling) in the sodium species transport scheme, then only sodium species are transported to the surface. This scenario would result in no increase in the barium-to-sodium ratio because the sodium species would either accumulate or equilibrate as carbonate with water to NaOH and CO_2. Therefore, barium salt buildup would not occur on the medium surface.

If, on the other hand, liquid salt viscous flow is significant, both Na_2CO_3 and $BaCO_3$ are transported to the surface. In this case, Na_2CO_3 will be the primary species vaporized, resulting in an increase in the barium-to-sodium ratio at the surface with an accumulation of barium salt at the pellet surface. This scenario will eventually result in partial choking of the surface capillary pores by the barium salt residue, thus diminishing with time the vaporization rate.

Analysis of pellets after thermal cycling tests shows higher carbonate content and higher barium-to-sodium ratio at the surface than the center of the pellets, thus indicating that volatilized carbonate from the surface is replenished by viscous flow of binary carbonate mixture

through the capillary structure of the MgO. The analysis also shows that the salt-rich layer at the pellet surface is very thin.

Pellet samples that underwent three phases of media performance tests were analyzed to confirm the salt migration trends. These samples were obtained from the center of the bed but at different height locations. The Na_2CO_3/MgO ratios indicate Na_2CO_3 depletion from the bed's topmost pellets but not from pellets at other locations. The Na_2CO_3/MgO ratio is higher for the medium located above the center and lower for the medium located below, a trend suggesting $BaCO_3$ migration from the bottom to the top of the bed as previously observed. The average composition of the tested pellets is in good agreement with that of the pretest composition and is in line with the small overall weight losses of the medium. These results indicate that Na_2CO_3-$BaCO_3$/MgO medium operated at 810°C or higher as the top pellets in the performance tests were subject to Na_2CO_3 loss. The $BaCO_3$ enrichment of the top pellet medium indicates that as Na_2CO_3 is lost from the top medium, it is being replenished by the advancing eutectic salt and not by the Na_2CO_3 component alone.

The next phase of this program includes a detailed technical and economic analysis of the Na_2CO_3-$BaCO_3$/MgO composite material as a storage medium for periodic kiln application in the brick/ceramic industry. This analysis will be undertaken by a subcontractor who is familiar with the equipment used by the industry and has experience in system design for the brick-making process. Further development of the material will be dependent upon the outcome of this assessment.

2.2.4 Form stabilization, high-density polyethylene (Project 2.7.1)

In previous research the University of Dayton Research Institute (UDRI) developed cross-linked, high-density polyethylene (HDPE) as a thermal storage material.[32] The HDPE was cross-linked by electron beam radiation to give a thermally form-stable material that melted at ~271°F and had a latent heat of fusion of 40 to 50 cal/g. At its melting point, the cross-linked HDPE changes from a white, opaque solid to a transparent, visco-elastic liquid. Repeatedly cycling through the melting point showed that the material melts and freezes congruently and has the basic

properties required for the storage of thermal energy for home heating and cooling.

The thermally form-stable property of HDPE is dependent on the extent of cross-linking. In their uncross-linked condition polyethylene pellets will melt and fuse together into one single, solid mass. After the pellets are cross-linked, they retain their shape when heated above their melting point and do not fuse together.

The heat of fusion of polyethylene is dependent on the linear carbon chain length and its crystallinity and molecular weight. The highest heat of fusion is obtained for high-density, linear, highly crystalline polyethylenes that have medium molecular weights. Cross-links are branch points that decrease the linear carbon chain length, the crystallinity, and the heat of fusion. Therefore, cross-linking must be kept to a minimum. Fortunately, this problem is not a serious one because one cross-link per molecule of 2000 carbon atoms is sufficient to eliminate melt flow.

Polyethylene pellets were irradiated with total doses of 2 to 12 mrad with an electron beam. Tests of these materials at various temperatures showed that total doses of 6 to 8 mrad were sufficient to ensure that the polyethylene pellets would retain their shape above their melting point. At total doses of 6 to 8 mrad, the pellets adhere but could be broken apart, and the mass did not hinder the flow of heat-exchange fluids. At higher doses of 12 mrad, the pellets did not adhere, but their heat of fusion was less than the 6-mrad material. Therefore, UDRI decided that a dose of 6 mrad would provide a material with an adequate thermal form stability and have a higher heat of fusion than the 12-mrad material, and 15,000 lb of the 6-mrad material was prepared and delivered to DOE.

Subsequent tests by other investigators showed that the material provided to DOE fused to a single mass that could not be broken apart and, thus, hinder the flow of the thermal exchange fluid. These investigators were using high-pressure steam as the heat-exchange fluid, and the effects of steam and high pressure on the pellet bed were not experimental conditions tested by UDRI.

UDRI, therefore, reexamined the processing conditions necessary to obtain satisfactory form stability for large-scale storage system operating conditions. Radiation dose was the principal variable to be investigated. However, contrary to estimates obtained previously of gamma (cobalt 60) radiation costing considerably more than electron beam radiation, the reverse was indicated as this program was initiated. Since the end results of electron beam and gamma irradiation are known to be the same (cross-linking by free radicals), both procedures were included for a comparison of the resulting material.

Small-scale laboratory screening tests were conducted to determine the final processing required. Two commercial HDPEs were selected for screening: the Alathon 7040, which was selected in the previous research as the final material, and Marlex 6006, a material with higher uncross-linked heats of fusion and crystallization. Initial tests uncovered another important processing variable for the gamma-irradiated material. The long exposure resulted in excess oxygen diffusion with a resulting high level of pellet-to-pellet adhesion. Therefore, irradiation under an inert atmosphere N_2 and under vacuum were added to the program.

Table 5 shows the complete series of processing conditions producing test samples for screening tests.

Table 5. Schedule of cross-linking processing of samples of polyethylene pellets

Electron beam radiation air (mrad)	Air (mrad)	Gamma radiation air N_2 (mrad)	Vacuum (mrad)
	4		
	6		
	8		
	10	2	10
6	10 black	3	12
8	12	4	
10	14	5	
12	16	6	
14	18	8	
		10	
		12	

The results of the screening tests resulted in the selection of Marlex 6006 as the material for further testing. The optimum processing chosen was a dose of 10 mrad of gamma radiation under a nitrogen atmosphere. Other results of the screening process are the following:

1. When processed by electron beam or gamma irradiation, under otherwise identical conditions, Marlex 6006 consistently provides better thermal form stability than Alathon 7040. The reasons for this difference in the response of the two commercial HDPEs to irradiation cross-linking are unknown at this time but may be due to differences in the stabilizers, antioxidants, or the amount of residual vinyl unsaturation in the two high-density polyethylenes. Vinyl unsaturation is known to be higher in the Marlex HDPE, and this would tend to promote better cross-linking.
2. Electron beam irradiation in air to a total dose of 10 mrad or higher will provide pellets of significantly better thermal form stability than those processed in prior DOE-sponsored research at 6 mrad.
3. When the irradiation is done in an air atmosphere, electron beam is superior to gamma. In fact, satisfactory thermal form stability was not achieved by gamma irradiation at any dose up to and including 18 mrad.
4. Gamma irradiation in an N_2 atmosphere, to a dose of 6 to 10 mrad, produced cross-linked HDPE pellets of superior thermal form stability and of better stability than those electron beams irradiated at the same dosage.
5. Gamma irradiation in a "vacuum" atmosphere provided slightly less thermal form stability than irradiating in N_2 but was superior to electron beam irradiation at comparable doses.
6. The incorporation of ~5 wt % of carbon black into Alathon 7040 and Marlex 6006 pellets did nothing to enhance the thermal form stability of pellets irradiated by gamma in air to a total dose of 10 mrad.
7. Preliminary, but still incomplete, data on the TES of electron beam and gamma irradiated pellets of Alathon 7040 and Marlex 6006 showed the expected reduction in ΔHF and ΔHc values for the lowest doses tested. However, increasing the dose to higher levels produced

little or no further change (decrease) in ΔHf and ΔHc properties. This latter finding was not expected, and the remaining experiments, when completed, should clarify this point.

A large sample of pellets will be further tested in the UDRI thermal test unit. A packed bed of 250 lb of material will be subjected to thermal cycling (with an ethylene-glycol-based heat transfer fluid) between 140 and 40°C. Thus, the material will be cycled through its 130°C melt temperature. If the tests are, as is expected, successful, this material will once again be made available for system tests to user agencies and industry.

2.3 TES System Development

Two projects concentrated on the definition of complete systems. In these cases, the performance of TES material is so closely tied to the complete system characteristics that independent development of storage is not meaningful. Both projects address passive solar heat storage, one seasonal and the other diurnal. To be meaningful, the dependence of storage performance on the specific solar building or other structure configuration requires development of an integrated system. Other research has addressed the question of generic application of these systems to a range of passive solar situations.

2.3.1 Ice/clathrate system for seasonal application (Project 3.1.1)

Studies by ANL[33] have shown the economic and technical feasibility of seasonal ice storage in the colder regions of the United States. A unique system that utilizes heat pipes to transfer seasonal cold to freeze ice in a storage tank has been successfully tested previously. A study was conducted to determine the economics of extending the period of cool storage through the higher freezing temperature allowed by clathrate rather than ice storage. The concept is to store cool in ice when the ambient temperature allows and in a clathrate when higher ambient temperatures prevail. Thus, a hybrid system would be utilized.

The economic study showed that clathrates of fluorocarbon, such as studied for diurnal cool storage, are not economical because of the large inventory of refrigerant required for seasonal storage. A search for a less expensive clathration material identified SO_2 as the lowest cost clathrate-former that could be considered for this service. The overall performance and cost appraisal still did not appear favorable enough for further research effort.

2.3.2 Advanced passive solar building materials (Project 3.1.2)

The search for effective applications of latent heat storage to solar building requirements led last year to the heat storage wall-panel concept. A Phase I study[34] looked at three different salt hydrates and three different plastics for the containment panels and concluded that the use of integral, PCM-filled wall panels was a practical, near-term alternative for passively storing and retrieving solar energy.

Thus, a Phase II program consisting of a test of full-scale prototype panels in a solar direct-gain and convection test chamber was initiated. System-level tests of prototype panels allowed measurement of system operating characteristics of realistic configurations. The tests, combined with subsystem tests, also will serve to provide data for validation of PCMSOL and other direct-gain computer simulation programs.

Subsystem tests of small, 1.5-ft^2 panels subject to ambient insulation were completed. Tests were of the following PCMs and channel sizes:

1. 1/4-in. channels filled with TESC 81,
2. 1/2-in. channels filled with TESC 81,
3. 1-1/2-in. channels filled with TESC 81,
4. 1/2-in. channels filled with $LiNO_3$ $3H_2O$,
5. 1/4-in. channels filled with n-Octadecane,
6. 1/2-in. channels filled with n-Octadecane,
7. 1/2-in. channels filled with Neopentylglycol, and
8. 1/2-in. channels filled with water.

Representative data from these tests, shown in Figs. 30–32, are from the panels with 1/2-in. channel width and height and contain TESC 81, calcium

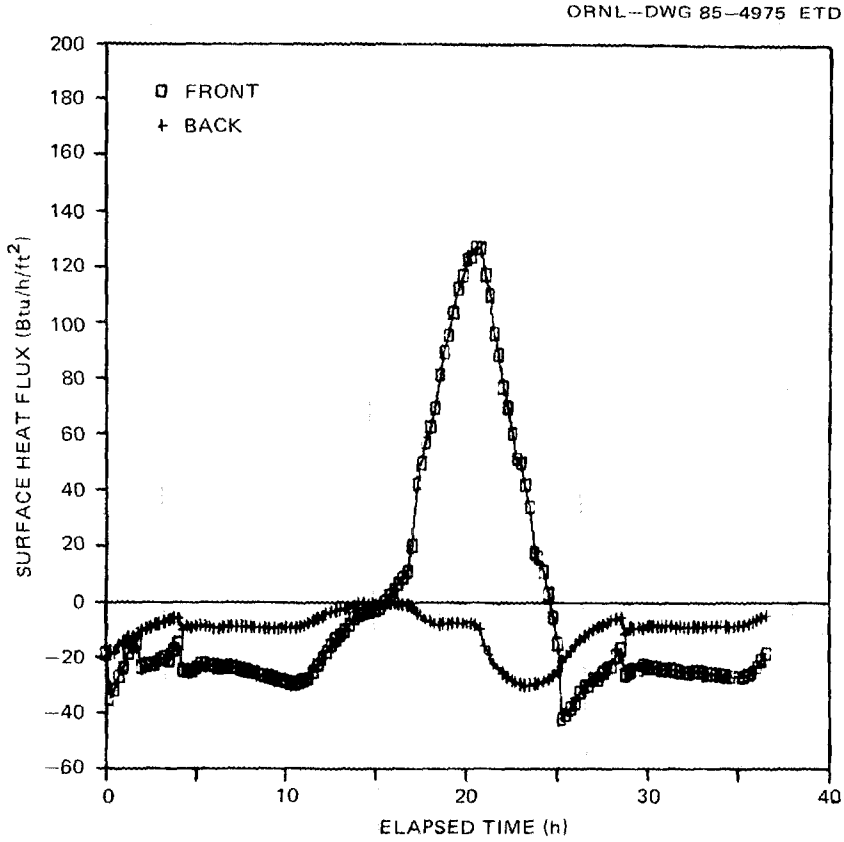

Fig. 30. Measured heat flaws.

chloride hexahydrate with additives, a commercial product of Dow Chemical. Figure 30 shows the heat flux to the panel over a 36-h period. Energy is being lost from the back of the panel over the complete time period. The period of sunlight is clearly indicated by the higher positive flux to the panel front. Figure 31 is the measured front and back surface temperatures for that panel over the same test period. The PCM was initially melted, and the freezing period of latent heat storage is seen between 5 and 12 h. A short period of supercooling is seen at the start of the freeze period, and the occurrence of phase change over a temperature range as found in the previous year's work is readily apparent from the falling surface temperatures over the freezing period. Figure 33 shows the effect as measured in the previous test program. The temperature at which the material receives (or loses) heat is shown to be spread over a range rather than to be discrete.

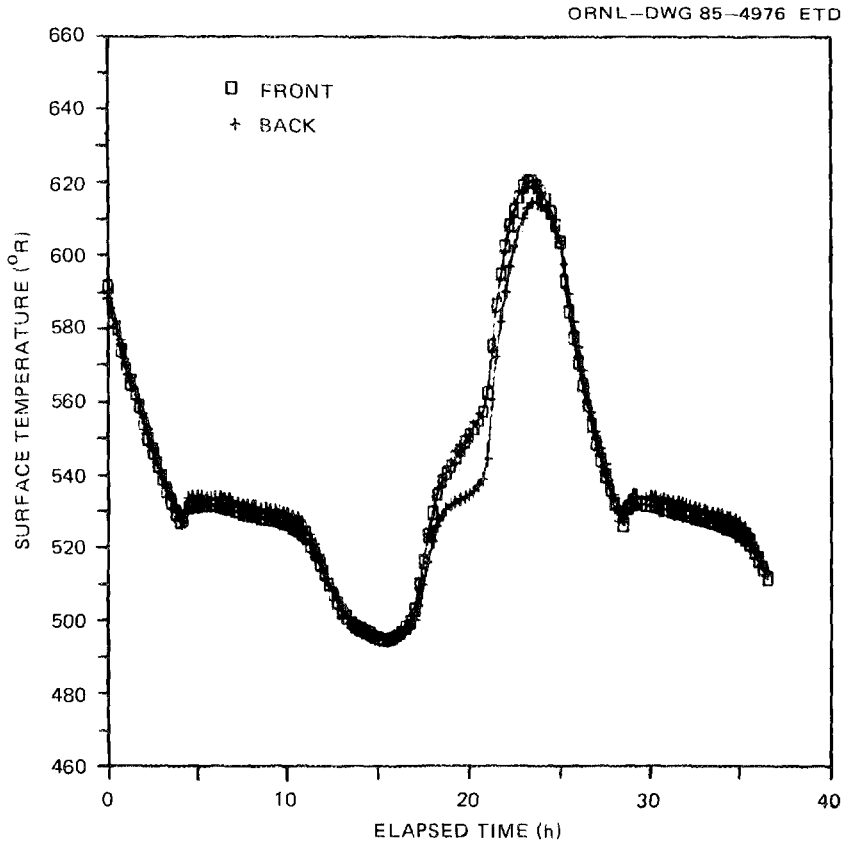

Fig. 31. Measured surface temperatures.

PCMSOL assumes the phase change is at a discrete temperature. The effect of this assumption is seen in Fig. 32, where the calculated response of the panel to the measured heat flux is shown. No supercooling is recognized by PCMSOL, and the freezing/melting is shown to be isothermal. Thus, the experimental data have shown the need for modifications to the modeling of this PCM, and such modifications are being incorporated into PCMSOL. The actual phase change temperature is seen in Fig. 31 to be ~30°C rather than the 36°C input to the computer run.

The computer simulation also fails to show cooling of the PCM below the transition temperature, that is, that all of the solar flux was absorbed in freezing the PCM. This failure is the result of a faulty input consisting of too large a value for heat of fusion for the PCM. The subcontractor developed a computer model that differs from PCMSOL in several ways but principally is a thermal network model.

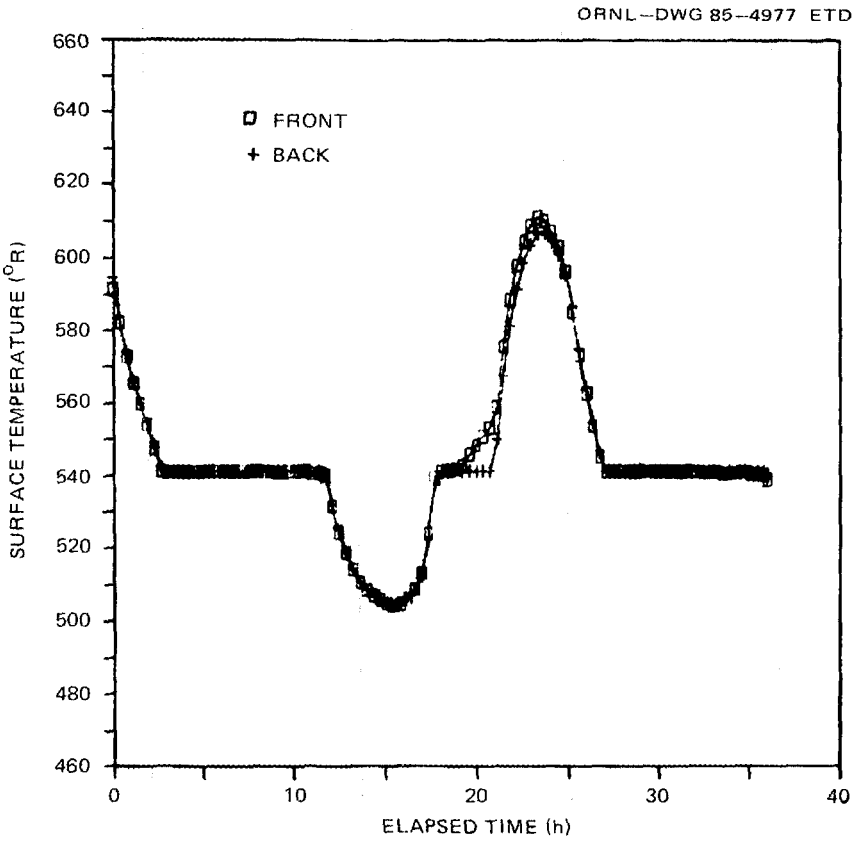

Fig. 32. PCMSOL calculated surface temperatures.

The thermal model of the PCM assumed uniform melting across the panel with no melting front. This assumption has been substantiated in tests for PCM up to 1/2 in. thick.

In the thermal analysis used, the energy stored must be expressed as a product of a specific heat and a temperature change. The gradual phase change exhibited by the TESC-81 lends itself to representing the heat of fusion as a temperature-dependent, apparent specific heat. The partial derivative of the energy stored obtained from test data (shown in Fig. 33) was calculated as a function of temperature and is shown in Fig. 34.

A comparison by PCMSOL of (1) calculated surface temperatures of a 1/2-in. panel containing TESC-81 and (2) this thermal analysis (TA) is shown by comparing Figs. 32 and 35. Again, the actual PCM melt temperature is not 81°F as assumed in the model but, rather, ~74°F. Subcooling

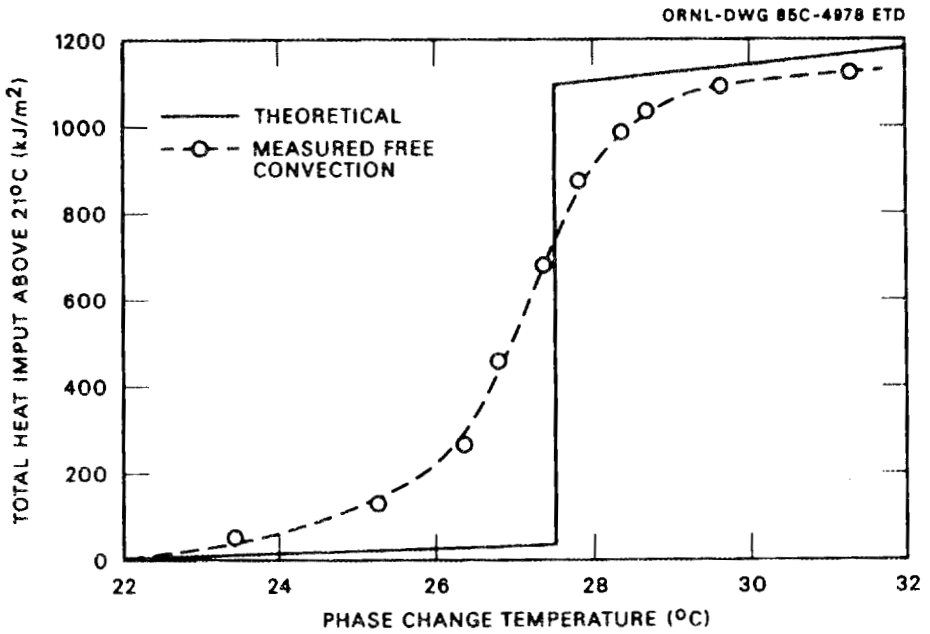

Fig. 33. Energy stored in TESC-81 as a function of PCM temperature.

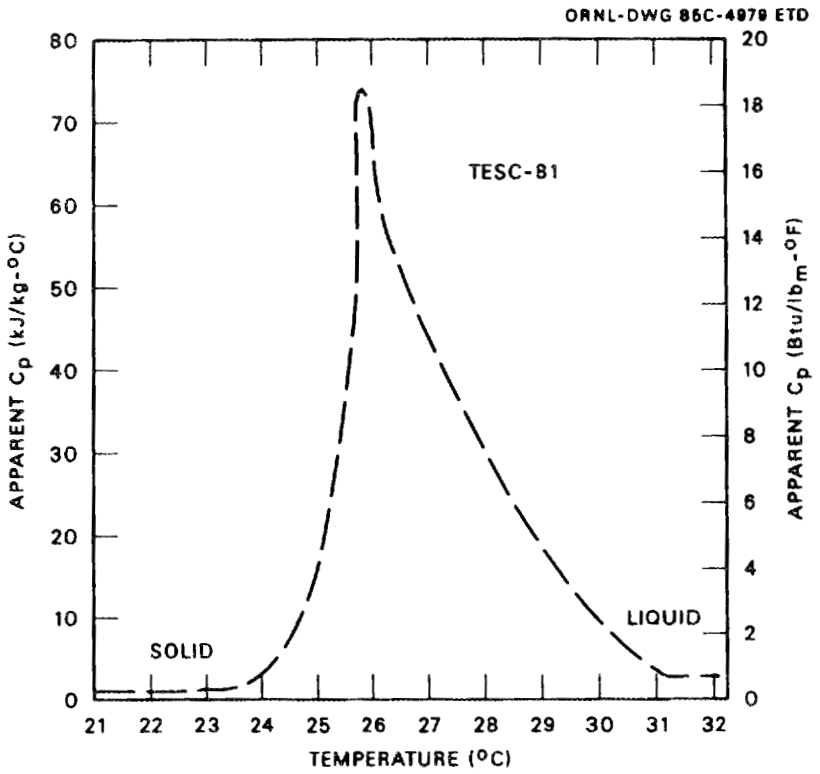

Fig. 34. Experimentally derived apparent specific heat of TESC-81 in plastic panels.

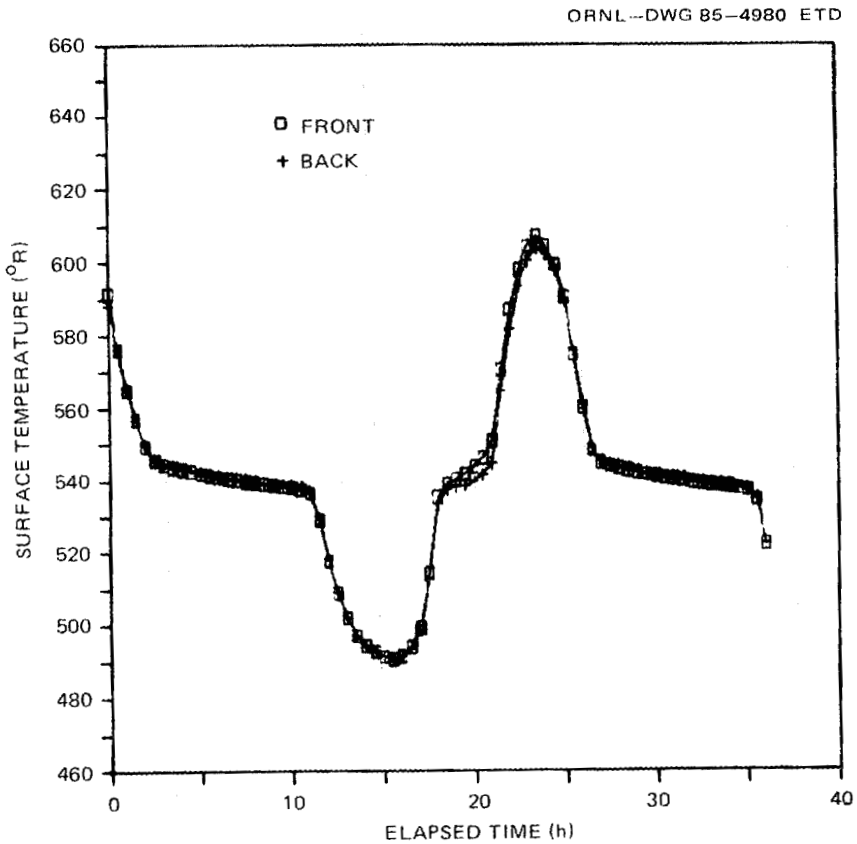

Fig. 35. Thermal-analyses calculated surface temperatures.

occurred (Fig. 31) at the start of both freeze cycles; melting and freezing obviously occurred over a temperature range rather than isothermally. The thermal analysis simulation, because it accommodates the last phenomenon, does show a drop of temperature over the freezing period. If the correct transition temperature had been used in the simulation, the model results would closely predict the test data. Furthermore, incorporation of a temperature range for melting and freezing in PCMSOL will bring together the two simulation results.

A preliminary economic analysis was performed. To perform any such detailed economic analysis, two important factors must be accurately determined for a new concept product: (1) manufactured/installed cost of the product and (2) worth of the product. However, early stages of development for a product such as PCM-filled panels preclude accurate determination of either of these factors.

There are several likely manufacturers of a product such as the PCM-filled panel. The most likely include the extruded plastic panel manufacturers, as well as manufacturers of PCM. Ideally, one company would manufacture all components to minimize product cost through the elimination of multiple profits and redundant costs. Major components should be purchased as raw materials and manufactured at one site to minimize the cost. In reality, however, this is not likely to be the case. For the purpose of this analysis, it was assumed that the manufacturer of the most expensive component (extruded plastic panel) would, therefore, purchase all other components in mass quantity and fabricate the final product at the plastic extrusion facility. Phone quotations for mass quantity buys were obtained for all components. A profit margin of 30% was assumed for the plastic panels and applied to the finished panel cost. An extra 10% was assumed for the panel cost to allow for heat sealing and adhering the vapor barrier material. An additional $\$0.23/ft^2$ was added to the polypropylene panel cost to allow for a substrate material. It was also assumed that installation cost would be $\$0.05/ft^2$ for thin polypropylene panels and $\$0.10/ft^2$ for thicker acrylic and polycarbonate panels. A total installed cost was then calculated. The panel was assumed to replace dry wall in new construction, which costs about $\$0.30/ft^2$ finished out, so that a differential cost could be obtained. This differential cost must then be paid back in energy savings.

Determination of energy savings or annual worth of the panel was not accurately obtained. The computer simulations were not for an entire residence or commercial building and not readily comparable to conventional structures. More specifically, the energy savings are directly a function of the number of cycles the PCM completes. Data for a typical building geometry were not generally available, and the data available were not easily used. It was known from experimental data, however, that the panels were easily charged on good solar days and discharged overnight by free or forced convection. It was assumed for this analysis that the amount and placement of the PCM guarantee that each pound of PCM is cycled when the solar energy is available to charge it directly. For Albuquerque, New Mexico, 150 cycles/year were assumed. This may seem high at first glance but in reality may be conservative because heating

is required at least partially for 6 months/year and good solar days are abundant. For TESC-81, the heat of fusion is 82 Btu/lb, which equates to 12,300 Btu/year-lb or $0.12/year-lb at $10/MBtu fuel replacement cost. It should be noted that no credit has been taken for load leveling in the summer, spring, and fall. Though unknown at this time, the exact contribution or worth because of the load leveling during this period is believed to be substantial.

A summary of costs, PCM worth, and payback in years is delineated in Table 6. A 1-1/2-in. acrylic panel is included in the analysis to illustrate the variation (reduction) in cost with increased thickness. It is believed that panels up to 1-1/2 in. thick could be utilized in specific locations for direct-gain applications. Polycarbonate material is also included, although it is more expensive than acrylic and appears to have no significant performance improvements above acrylic. The 1/4-in. panels should not be considered for direct gain applications because of potential overheat for thin panels. Direct-gain tests revealed that the 1/4-in. panels will easily melt in <1 h in good sun and, therefore, should not be used as direct-gain panels. In summary, the paybacks range from ~3 years to 6 years (excluding polycarbonate) for heating only.

If PCM is added for passive solar heating reasons, then the opportunity for further beneficial use of the PCM presents itself every day that the ambient temperature swings above and below the comfort zone. Relatively simple and inexpensive techniques are available (e.g., vent and recirculation fans) to allow storing either heating or cooling energy from the ambient air during much of the spring, fall, and summer. This storage can significantly affect the economics of the PCM directly through reduced heating/cooling costs and indirectly through better temperature control and improved comfort.

Under conditions where the diurnal temperature variations do not permit storing "free" energy from ambient air, the PCM still has a potential benefit. Off-peak energy (at reduced rates) is presently not in widespread application. However, the use of computers for monitoring power use could change this relatively soon. If this occurs, the use of PCMs to store energy generated by heat pumps during off-peak times can be

Table 6. Economic worth/payback analysis

Component or cost factor	Cost ($/ft^2)			
	1/4-in. Polypropylene	5/8-in. Acrylic	5/8-in. Polycarbonate	1-1/2-in. Acrylic
Extruded plastic	0.19	1.48	2.28	2.38
Added cost to panel for sealing and adhering vapor barrier	0.02	0.25	0.23	0.24
PCM TESC-81	0.10	0.29	0.29	0.80
Vapor barrier	0.10	0.05	0.05	0.05
Substrate	0.12			
Total materials cost	0.53	1.97	2.85	3.47
30% Profit	0.12	0.55	0.79	0.97
Installation labor	0.15	0.10	0.10	0.10
Total installed cost	0.70	2.62	3.74	4.54
Replaced materials	−0.30	−0.30	−0.30	−0.30
Differential costs	0.40	2.32	3.44	4.24
Worth of PCM panel, $/ft^2-year	0.12	0.36	0.36	0.98
Payback (heating only), years	3.3	6.3	9.2	4.3

very cost-effective, particularly when the effect of increased COP (because of more favorable operating conditions) is considered.

2.4 Technology Transfer of Solid Sensible Heat Storage Material (Project 4.3.1)

Olivine heat storage bricks for electric storage furnaces are presently imported from Europe. Two recently completed material development projects under this program have made technologies for producing such

bricks available to U.S. industry.[35,36] The fabrication methods that have been developed circumvent the high equipment cost required for the presently used ceramic bricks. However, to replace the existing method, lower technology requirements and less energy-intensive methods have been developed in ram-pressed and cast bricks utilizing various cementing materials that do not require high firing temperatures in the fabrication process. Thus, the technology can be utilized by small industrial firms. Large deposits of olivine suitable for these bricks exist on both the east and west coasts.

The fabrication technology, prototype sample bricks, and, in one case, experimental fabrication dies, along with results of tests of the prototype brick performance in storage heaters, have been made available to the private sector.

Storage heaters have resistive heating elements that generate heat to be stored in a ceramic refractory core, which is heated to temperatures up to about 800°C during off-peak periods. During peak periods the heaters use forced convection to transfer the stored heat to the environment. In the past the cores have been constructed from conventionally pressed and fired (sintered) bricks of magnesite (magnesium oxide) or olivine (magnesium silicate) compositions. Research completed this year has shown that both fired brick based on North Carolina olivine and chemically bonded, pressed brick based on Washington State olivine have potential use in storage heater cores.

In this project, chemically bonded concretes (i.e., slurry castables) based on North Carolina olivine aggregates were developed for use in refractory cores of storage heaters. Chemical binders used were calcium aluminate cements and sodium polyphosphate. Additions of high specific gravity minerals such as magnetite (millscale) produced concrete components with densities equaling those of conventionally fired brick. This result implies that volumetric heat capacities of fired olivine brick and of olivine castables may be the same, depending on the concrete composition.

In a 50-cycle test program in a commercial, 15-kW, room-size storage heater, the calcium aluminate, cement-bonded, olivine castable exhibited

no degradation because of the cyclic thermal environment. Larger concrete sections cast about the resistive heating elements showed no degradation, and there was no difference in the heater's performance with cement-bonded components as compared with fired-brick components. The cement-bonded components were limited to local service temperatures below about 1200°C (about 2200°F). The phosphate-bonded castables can be used above 1200°C, but they were found to be more susceptible to thermal shock damage.

This research work has demonstrated that low-cost concretes based on domestically available olivine aggregates can be used to construct heat storage cores. Relatively simple concrete casting and curing techniques can be used to produce those cores. There is no significant capital investment requirement, suggesting that small business concerns could participate in the fabrication of heater cores. The technologies for producing refractory olivine concretes can be rapidly commercialized for night storage heater and other TES applications.

2.5 System Modeling

2.5.1 Passive solar building modeling (Project 5.1.1)

TES is an essential component of passive solar buildings, allowing solar energy received during the day to be converted to heat and stored for building heating at night. The heat, whether stored in an intentionally added building component such as a Trombe wall or the sum of heat stored in the normal building elements, is, along with the collector, the passive solar heating system. Conventional solar technology has relied on sensible heat storage in rocks, masonry, etc. The advantage of latent heat storage in compactness of the storage media, as well as in possible increased room thermal comfort as a result of isothermal storage of energy, is recognized and beginning to be exploited in commercial systems. The advantages seen from the use of the latent heat of PCMs are

1. storage of large amounts of heat per unit mass or per unit volume as the latent heat H (kJ/kg) of phase change;[37-43]
2. the temperature range over which heat is stored can be narrow, so long as it spans the phase change temperature T_{cr} (°C);[44-46]

3. conditions can be created under which the PCM temperature will be T_{cr} for most time;[30,32] and
4. PCM storage can be "passive."[33-35]

These advantages may, however, be of illusory value. For example, if T_{cr} is too high or too low, the phase change will not take place, and latent heat will not be stored. Similarly, if too little PCM is used, the phase change process may be ineffective. On the other hand, too much PCM may not be cost-effective or practical. Also, the phase change process must be driven by thermal fluxes large enough to provide heat of magnitude greater than the latent heat.[35] Therefore, where and how the PCM is placed are very significant in a passive storage mode. These considerations imply the necessity of optimizing the way in which PCM is used with respect to a number of variables, including

1. PCM choice,
2. PCM placement,
3. PCM geometry, and
4. cost.

A tool that can be used to address this need is a valid computer simulation program, applicable to a sufficiently general family of structures. PCMSOL-1, a code that simulates a one-room structure in which PCM may be incorporated by wall layers, was developed previously under this program.[47] This year the code was validated against solar test cell data (Sect. 2.3.2). The code was used in an analysis of the relationships between storage performance and PCM thermophysical parameters. This was a preliminary study in a program aimed at determining criteria for development of passive solar storage components that utilize the latent heat of storage media.

In this preliminary analysis, a PCMSOL simulation of a one-room passive solar building with various PCM storage configurations was utilized. In an effort to bypass the computing time required for extensive simulations of annual room performance, the following method was used.

1. Peak-day supplemental heating was determined over a range of PCM parameters and storage locations in the room.

2. Annual supplemental heating was projected from an assumed daily supplemental energy requirement over the heating season related to the three peak-day requirements (Fig. 36).
3. Allowable PCM storage system costs were determined based upon these predictions.
4. Preliminary criteria for development of latent heat storage elements were then determined.

The peak daily heating requirement was expressed in terms of nondimensionalized PCM properties as

$$\text{Peak-day heating required} = A_0 + A_1\rho^* + A_2H^* + A_3T^* + A_4K^* + A_5L^* + \text{2nd order terms} , \quad (15)$$

where

$$\rho^* \text{ (nondimensionalized density)} = \frac{\rho - 95}{120 - 70} ,$$

$$H^* \text{ (nondimensionalized latent heat)} = \frac{H - 80}{100 - 60} ,$$

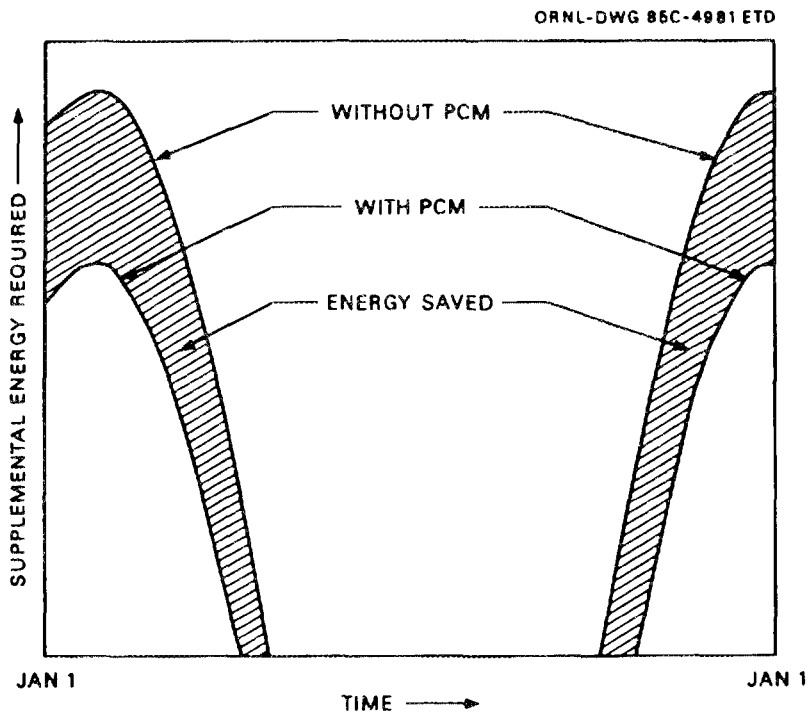

Fig. 36. Peak day related to annual energy use.

$$T^* \text{ (nondimensionalized melt temperature)} = \frac{T - 82}{90 - 75},$$

$$K^* \text{ (nondimensionalized conductivity)} = \frac{K - 0.3}{0.6 - 0.1},$$

$$L^* \text{ (nondimensionalized thickness)} = \frac{L - 1.2}{2 - 0.25}.$$

Sensitivity analysis of the peak-day simulation with variations in the above parameters gave optimum PCM properties for each location in the room simulated. Allowable costs can then be determined from assumptions of energy cost, escalation, and discount rate (Fig. 37).

This program will continue with a systematic evaluation of typical storage systems and media.

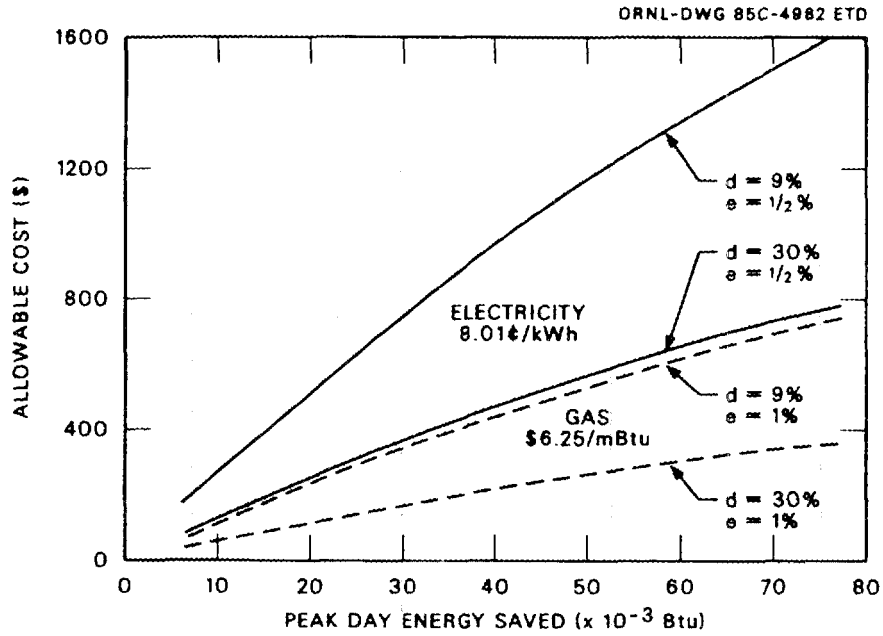

Fig. 37. Range of allowable cost for PCM storage system.

2.5.2 Mathematical modeling of a PCM system (Project 5.2.1)

An analytical study to develop a mathematical model of two-phase flow over a packed bed and an experimental program for model verification was completed.[48]

The previous year's experimental work with PWC-89 pellets of encapsulated Glauber salt subject to R-12 heat transfer fluid uncovered deficiencies in permeability of the pellet skin. Further tests of an improved pellet, using a heat transfer fluid, R-113, with a lower saturation pressure, were only marginally successful. Thus, experiments were continued with glass spheres substituted for pellets of PCM. The results of the experimental runs provide heat transfer correlations for liquid R-113 flow and two-phase liquid-vapor flow for use in the developed computer code.

The mathematical model has been developed to simulate transient thermal performance of a packed bed of encapsulated PCM pellets using a refrigerant as the heat transfer fluid. The governing equations were developed for three general conditions of progressively increasing complexity:

1. No phase change occurs in either the working fluid or the PCM pellets. This condition represents conventional TES storage in a packed bed.
2. Phase change occurs in the pelletized PCM but not in the working fluid. This condition represents two very general operating conditions. The first of these, an initially frozen PCM packed bed that is at an initial temperature below the melting temperature of PCM (t_m), is heated with a single-phase heat transfer fluid entering the bed at a temperature above t_m. In this general heating case, the PCM initially undergoes sensible heating of solid, then melting, and finally sensible heating of liquid PCM. The second of these, an initially liquid PCM in the bed at a temperature above t_m, is cooled with a single-phase heat transfer fluid entering the bed at a temperature below t_m. In this general cooling case, the PCM liquid initially undergoes sensible cooling, then freezing, and finally sensible cooling of solid PCM.
3. Phase change occurs both in the working fluid and the pelletized PCM.

The heat transfer correlation derived from liquid R-113 flow runs is also applicable to R-113 vapor flow. For the heat transfer between the

heat transfer fluid (R-113) and the bed wall, the correlation of Yagi and Kunii[49] for air as the working fluid is modified for use with R-113.

The heat transfer fluid used in the single-phase working fluid runs was R-113. The bed packing material used was 5/8-in.-diam, smooth, glass spheres. Both "heating" and "cooling" runs were made at flow rates ranging from 0.25 to 4 gal/min. In the "cooling" runs the glass spheres were first heated by running hot refrigerant through the packed bed at a flow rate of 4 gal/min for 1 h to achieve a uniform initial bed temperature. Then the bed was isolated by closing the solenoid valves at the two ends of the bed, and the working fluid was then cooled to the desired bed inlet temperature in a bypass loop prior to the beginning of a test-run. In all of the "cooling" runs, the tube-and-shell heat-exchanger, coolant-water flow regulating valve was set to the full-open position. The power input by electrical heating to the working fluid was typically considerably higher than the rate of energy absorption of the packed bed. The excess energy input was removed on the tube-and-shell heat exchanger. The purpose of this procedure was to reduce the time-dependent fluctuation in bed inlet temperature. In most runs the working fluid flow direction was downward through the packed bed. At low flow rates, 0.5 gal/min or less, natural convection effects were found to be important, and it became necessary to use upflow through the packed bed to avoid working-fluid flow reversals in "cooling" runs and downflow through the bed in "heating" runs. Prior to the beginning of each heating run, the bed inlet diffuser was heated on the outside with a heat tape until the inlet temperature of the working fluid reached the desired value. This was done to achieve a steeper step in the bed inlet-temperature curve. With the exception of the diffuser heating, the basic procedure followed in the "heating" runs was similar to that followed in the "cooling" runs.

The heat transfer fluid used in the two-phase working fluid runs was also R-113. Five cases of bed inlet quality were used, ranging from 0.24 to 0.94. In all of the two-phase working fluid runs, the flow direction was downward through the bed. Prior to beginning a two-phase run, the bed was brought up to steady state by running two-phase refrigerant of the desired inlet quality through the bed. For each two-phase run, data

were recorded at three different power levels of the heat flux probes to determine the influence of the temperature difference between rod surface and working fluid on the heat transfer coefficient. Typically, data were recorded for 1 h at each power setting.

Some comparisons of numerical predictions with experimental results are shown in Figs. 38 and 39. These results show excellent agreement and validate the first stage of the modeling effort. Data correlations for the more complex model, that is, with phase change in the storage material, must await development of a more reliable encapsulation process.

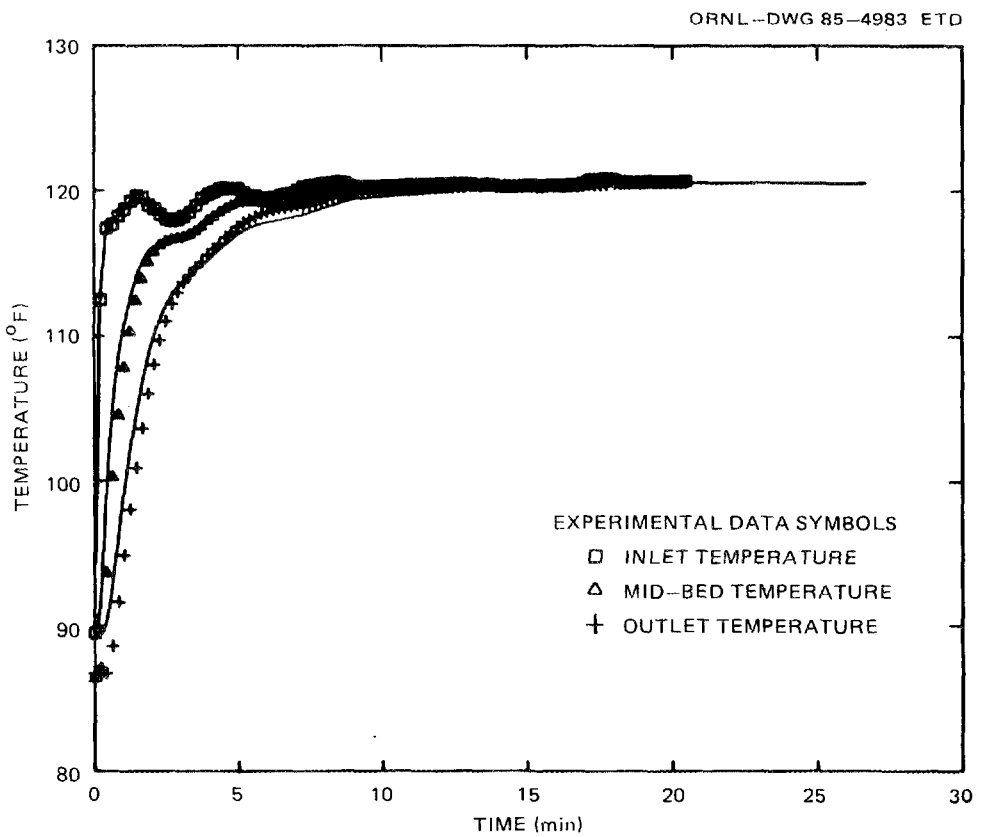

Fig. 38. Comparison of experimental data with numerical predictions, heating.

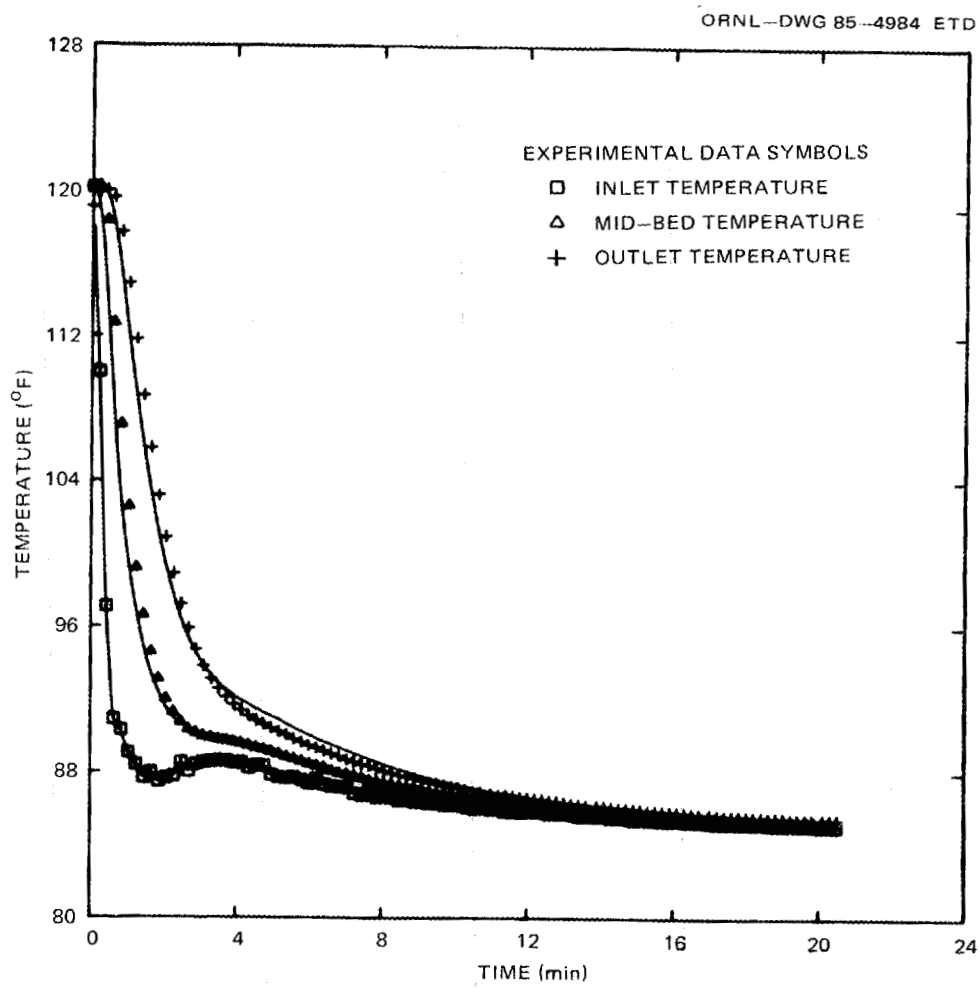

Fig. 39. Comparison of experimental data with numerical predictions, cooling.

3. SUMMARY AND CONCLUSIONS

Technical progress in the development of advanced TES systems for the period of April 1983–March 1984 has been presented. Each of the ORNL/TES program activities during this period has been summarized, and references to detailed reports of specific projects have been given. In accordance with DOE guidelines, the program has continued during this seventh year of ORNL participation as long-range and generic technology development.

An economical method of fabricating a composite ceramic-salt material for high-temperature latent heat storage in a packed bed has been demonstrated. This class of storage media will allow the latent heat of fusion of the salt to be utilized for heat storage without the necessity of containing the salt as a liquid in the storage vessel. Some research into the mechanism of thermally cycled salt migration out of the composite material remains to be conducted. However, the concept is shown to be sufficiently successful that a detailed economic study of its use in industry has been scheduled as the follow-up phase of this project.

Studies of methods for encapsulating metallic eutectic alloys in nonreactive metallic shells were initiated. Many of these alloys that have high heats of fusion at high temperatures are excellent candidates for storage of industrial reject heat. The successful development of an encapsulation process has potential for wide application. Although this year's efforts have not produced a successful method, further research remains as part of the TES program.

Successful demonstrations of TES cycles for use with heat pumps have been achieved. A clathrate of mixed fluorocarbons that forms at near ideal storage temperature and pressure for air conditioning was identified through in-house laboratory studies. A subcontracted effort in pursuit of a dual-season storage medium for the heat pump circuit is achieving some success, and further laboratory studies are recommended.

Research aimed at establishing phase data for selected systems that can store energy in heats of solution and mixing will continue. One promising system has been identified for further study.

The ORNL passive solar computer code PCMSOL was validated through comprehensive experiments conducted in solar test cells. The code is now being applied to the probe of identification of latent heat storage concepts that promise success. This ongoing mathematical modeling effort has proven very helpful in understanding the difficult problem of capturing and using solar heat in a passive system.

REFERENCES

1. J. L. Atwood and W. J. Schaetzle, *Dual Temperature Hydrates for Heat Pump/Latent Heat Storage Applications*, University of Alabama, to be published.

2. W. Nernst, *The New Heat Theorem*, Dover Publications, Inc., New York, 1969.

3. P. G. Grodzka, *Feasibility Study of Binary Solutions for Thermal Energy Storage in High and Low Temperature Applications*, ORNL/Sub/83-13858/1, Martin Marietta Energy Systems, Inc., Oak Ridge Natl. Lab., December 1984.

4. P. G. Grodzka, *An Initial Study of the Potential of Conjugating Binary Mixtures for Thermal Energy Storage*, Report LMSC-HREC TR D867240, Lockheed Missiles & Space Company, Huntsville, Ala., prepared under Battelle-Northwest Subcontract B-D5565-A-0 (prime contract DE-AC06-76RLO-1830), August 1983.

5. F. Franks, *Physico-Chemical Processes in Mixed Aqueous Solvents*, American Elsevier Publishing Company, Inc., New York, 1967, p. 54.

6. G. Jura et al., "Phenomena in the Liquid-Liquid Critical Region," *Proc. Nat. Acad. Sci. USA* 39, 19–23 (Jan. 15, 1953).

7. K. Govindarajan, B. Viswanathan, and E. S. R. Gopal, "The Heat Capacity of Liquid Carbon Disulfide + Acetonitrile, Especially Near the Upper Critical Solution Temperature," *J. Chem. Thermodyn.* 5, 73–81 (May 1975).

8. M. P. Ternes, "Studies on the R-12 Gas Hydrate Formation Process for Heat Pump Cool Storage Applications," *Proceedings of the DOE Physical and Chemical Energy Storage Annual Contractor's Review Meeting*, 12–14 September 1983, CONF-830974, Union Carbide Corp. Nuclear Div., Oak Ridge Natl. Lab.

9. D. W. Davidson and S. R. Gough, "Composition of Tetrahydrofuran Hydrate and the Effect of Pressure on the Decomposition," *Can. J. Chem.* 49, 2691–99 (1971).

10. J. J. Christensen, R. W. Hanks, and R. M. Izatt, *Handbook of Heats of Mixing*, Wiley, New York, 1982.

11. D. W. Davidson, "Clathrate Hydrates," p. 127 in *Water: A Comprehensive Treatise*, Vol. 2, ed. F. Franks, Plenum Press, New York, 1973.

12. M. E. Post et al., "The Excess Enthalpies of Seven (Propane + Alcohol) Mixtures at 298.15 K," *J. Chem. Thermodyn.* 13, 77–80 (1981).

13. N. F. Catherall and A. G. Williamson, "Mutual Solubilities of Propylene Carbonate and Water," *J. Chem. Eng. Data* 16(3), 335 (July 1971).

14. C. S. Hong et al., "Some Thermodynamic Properties of Systems Containing Propylene Carbonate and Ethylene Carbonate," *J. Chem. Eng. Data* 27(2), 146 (April 1983).

15. G. Jura et al., "Phenomena in the Liquid-Liquid Critical Region," *Proc. Nat. Acad. Sci. USA* 39, 19 (Jan. 15, 1953).

16. H. Schmidt, G. Jura, and J. H. Hildebrand, "The Heat Capacity of the System Carbon Tetrachloride-Perfluoromethylcyclohexane Through the Critical Region," *J. Phys. Chem.* 63, 297 (February 1953).

17. H. Klein and D. Woermann, "Specific Heat of Binary Liquid Mixtures Near the Critical Mixing Point," *Ber. Bunsenges. Phys. Chem.* 79(12), 1180 (December 1975).

18. M. Pelger, H. Klein, and D. Woermann, "Evidence of Hydrophobic Effects from Critical Phenomena," *Ber. Bunsenges. Phys. Chem.* 85(5), 356 (May 1981).

19. J-Y Cabon, M. L'Her, and M. Le Demezet, "Physical Properties of the Ethylene Carbonate-Water System at 40°," *C. R. Acad. Sci. Paris* 280, 747 (March 1975).

20. G. P. Cunningham, G. A. Vidulich, and R. L. Kay, "Several Properties of Acetonitrile-Water, Acetonitrile-Methanol, and Ethylene Carbonate-Water Systems," *J. Chem. Eng. Data* 12(3), 336 (July 1967).

21. M. L. Lakhanpal, S. C. Ahuja, and H. G. Mandal, "Thermodynamic Properties of Solutions of Ethylene Carbonate in Water, Benzene, and Chloroform at 298 K," *Indian J. Chem.* 16A, 928 (November 1978).

22. E. Zakirov, "Some Physicochemical Properties of the Ethylene Carbonate-Water System," *Nauchn. Tr. Tashk. Tekst. Inst.* (2), 209 (1967).

23. B. E. Geller, "Thermodynamic Properties of the System Ethylene Carbonate-Water," *Izv. Vyssh. Uchebn. Zaved. Khim. Khim. Tekhnol.* 5, 391 (1962).

24. J. J. Tomlinson, "Heat Pump Cool Storage in a Clathrate of Freon," pp. 2060–64 in *Proceedings: 17th Intersociety Energy Conversion Engineering Conference, Los Angeles, August 8–12, 1982*, Vol. 4, Institute of Electrical and Electronics Engineers, New York, 1982.

25. J. J. Tomlinson, "Clathrates — A Storage Alternative to Ice for Residential Cooling," *Opportunities in Thermal Storage R&D*, EM-3159-SR, ed. W. Hausz and B. J. Berkowitz, Electric Power Research Institute, July 1983.

26. M. P. Ternes, "Characterization of Refrigerant-12 Gas Hydrate Formation for Heat Pump Cool Storage Applications," American Society of Mechanical Engineers paper 84-AES-12, 7th Annual Energy Sources Technology Conference, New Orleans, February 12–17, 1984.

27. J. J. Carbajo, "A Direct-Contact-Charged, Direct-Contact-Discharged Cool Storage System Using Gas Hydrate," *American Society of Heating, Refrigerating and Air-Conditioning Engineers Meeting, Honolulu, June 23–27, 1985*, to be published in *ASHRAE Transactions 1985*, Vol. 91, Part 2B (February 1986).

28. J. J. Tomlinson et al., "A Comparative Study of Cool Storage Systems Based on Ice and Clathrates," pp. 1201–06 in *Proceedings of the 19th Intersociety Energy Conversion Engineering Conference, San Francisco, August 19–24, 1984*, Vol. 2, American Nuclear Society, La Grange Park, Ill., 1984.

29. F. D. Ferguson and T. K. Jones, *The Phase Rule*, Butterworth Co., London, 1966.

30. M. von Stackelberg and W. Meinhold, "Feste Gashydrate III: Mischhydrate," *Z. Elektrochem.* 58(1), 40–45 (March 1954).

31. A. Ananthanarayanan et al., *Hypereutectic Heat Storage Shot*, RF Project 763884/715844, Ohio State University Research Foundation, Columbus, Ohio, January 1985.

32. I. O. Salyer, *Development and Testing of Electron Beam Cross-Linked High-Density Polyethylene for Energy Storage*, University of Dayton, Dayton, Ohio, to be published.

33. G. J. Gorsky et al., *Ice Production and Storage for Seasonal Applications Utilizing Heat Pike Technology*, ANL-82-87, Argonne Natl. Lab., Argonne, Ill., September 1982.

34. J. W. Fletcher et. al., *Development of Heat Storage Building Materials for Passive Solar Applications*, ORNL/Sub/82-17460/1, Union Carbide Corp. Nuclear Div., Oak Ridge Natl. Lab., February 1984.

35. O. J. Whittemore, *Unified Olivine Heat Storage Media*, ORNL/Sub/81-9063/1, Union Carbide Corp. Nuclear Div., Oak Ridge Natl. Lab., October 1983.

36. D. A. Brosnan, *Chemically Bonded Ceramic Materials for Use in Thermal Energy Storage Devices*, ORNL/Sub/81-16953/1, Martin Marietta Energy Systems, Inc., Oak Ridge Natl. Lab., August 1985.

37. B. Carlson and G. Wettermark, "Heating-Transfer Properties of a Heat-of-Fusion Store Based on $CaCl_2 \cdot 6H_2O$," *Sol. Energy* 24(3), 239–47 (1980)

38. C. Christensen and D. Benson, *Advanced Phase-Change Storage: Analysis of Materials and Configurations*, SERI/TP-255-2018, Solar Energy Research Institute, Boulder, Colo., June 1983.

39. P. Grodzka, "Selection of Solid-Liquid Phase-Change Materials for Spacecraft Thermal Control," pp. 547–65 in *Heat Transfer and Spacecraft Thermal Control*, ed. John Lucas, Massachusetts Institute of Technology, Cambridge, Mass., 1971.

40. D. Hale et al., *Phase Change Materials Handbook*, Report NASA CR-61363, Lockheed Missiles and Space Company, Huntsville, Ala., September 1971.

41. S. Marks, "An Investigation of the Thermal Energy Storage Capacity of Glauber's Salt with Respect to Thermal Cycling," *Sol. Energy* 25(3), 225–58 (1980).

42. T. Ozawa, "Screening and Experimental Evaluation of Latent Heat Thermal Energy Storage Materials," pp. 53–56 in *Proceedings of the Third Japan Symposium on Thermophysical Properties*, 1982.

43. Y. Takahashi et al., "Investigation of Latent Heat-Transfer Energy Storage Materials. I. Thermoanalytical Evaluation of Modified Polyethylene," *Thermochim. Acta* 50, 31–39 (December 1981).

44. A. Soloman, "Design Criteria in PCM Wall Thermal Storage," *Energy* 4, 4701–09 (June 1979).

45. A. Soloman, *Mathematical Modeling of Phase Change Processes for Latent Heat Thermal Energy Storage*, ORNL/CSD-39, Union Carbide Corp. Nuclear Div., Oak Ridge Natl. Lab., August 1979.

46. S. Faunce and S. Rickert, "Measurement of the Heat Transfer Rate for Thermal Energy Storage Masses in Direct Gain Passive Solar Heating Systems," pp. 626–31 in *Solar Engineering — 1981*, American Society of Mechanical Engineers, New York, 1981.

47. G. A. Geist et al., *PCMSOL-1 — A Computer Simulation Code for a Direct Gain Passive Solar Structure*, ORNL/CSD-127/P1&P2, Union Carbide Corp. Nuclear Div., Oak Ridge Natl. Lab., February 1984.

48. R. V. Arimilli and A. G. Graves, *Liquid-Vapor Flow and Heat Transfer in a Packed Bed of PCM, Transient Thermal Performance*, University of Tennessee, Knoxville, Tenn., to be published.

49. S. Yagi and D. Kunii, "Studies on Heat Transfer Near Wall Surface in Packed Beds," *AIChE J.* 6(1), 97 (March 1960).

ORNL/TM-9819
Dist. Category UC-94a

Internal Distribution

1. T. D. Anderson
2. R. S. Carlsmith
3. D. M. Eissenberg
4. J. A. Getsi
5. P. A. Gnadt
6. H. W. Hoffman
7. S. I. Kaplan
8. R. J. Kedl
9. M. A. Kuliasha
10-14. J. F. Martin
15. J. W. Michel
16. W. R. Mixon
17. F. R. Mynatt
18. M. Olsewski
19. M. W. Rosenthal
20. A. C. Schaffhauser
21. A. Solomon
22. J. J. Tomlinson
23. H. E. Trammell
24. C. D. West
25. ORNL Patent Office
26. Central Research Library
27. Document Reference Section
28-29. Laboratory Records Department
30. Laboratory Records (RC)

External Distribution

31. Joseph G. Asbury, Argonne National Laboratory, 9700 South Cass Ave., Argonne, IL 60439
32. S. R. Bull, Solar Energy Research Institute, 1536 Cole Boulevard, Golden, CO 80401
33. E. J. Cairns, Lawrence Berkeley Laboratory, University of California, Berkeley, CA 94720
34. Howard Coleman, Office of Solar Heat Technologies, Department of Energy, Forrestal Bldg., CE 314, 1000 Independence Ave., Washington, DC 20585
35. Landis Kannberg, Battelle Pacific Northwest Laboratories, P.O. Box 999, Battelle Boulevard, Richland, WA 99352
36. Ken Klein, Office of Energy Storage and Distribution, U.S. Department of Energy, Forrestal Bldg., 1000 Independence Ave., Washington, DC 20585
37. Al Landgrebe, Office of Energy Storage and Distribution, U.S. Department of Energy, Forrestal Bldg., 1000 Independence Ave., Washington, DC 20585
38. Robert L. San Martin, Deputy Assistant Secretary for Renewable Energy, Department of Energy, CE-30, 6C-026/Forrestal Bldg., 1000 Independence Ave., Washington, DC 20585
39. Alessio Mezzina, Brookhaven National Laboratory, Upton, NY 11973
40. Allan Michaels, Argonne National Laboratory, 9700 South Cass Ave., Argonne, IL 60439
41. Dave Pellish, Department of Energy, Forrestal Bldg., Rm. 5H079, 1000 Independence Ave., Washington, DC 20585

42. Veronika A. Rabl, Electric Power Research Institute, 3412 Hillview Ave., P.O. Box 10412, Palo Alto, CA 94303
43. Office of Assistant Manager for Energy Research and Development, Department of Energy, ORO, Oak Ridge, TN 37831

44-201. Given distribution as shown in DOE/TIC-4500 under Category UC-94a (Energy Storage — Thermal)